Zeitschrift: IABSE reports = Rapports AIPC = IVBH Berichte
Band: 76 (1997)

Rubrik: Theme E: Fatigue testing

Theme E

Fatigue Testing

Leere Seite
Blank page
Page vide

Repair Techniques for the Rehabilitation of Fatigue Cracked Orthotropic Steel Bridges

Stefano CARAMELLI
Associate Professor
University of Pisa
Pisa, Italy

Stefano Caramelli, born in 1945, received his Civil Engineering Degree from the University of Pisa. He is currently Associate Professor of Structural Design at the Department of Structural Engineering of University of Pisa.

Pietro CROCE
Assistant Professor
University of Pisa
Pisa, Italy

Pietro Croce, born in 1957, got his PhD degree in 1989. He is Assistant Professor at the Department of Structural Engineering of University of Pisa. He is involved in several researches on bridges, fatigue and reliability.

Maurizio FROLI
Assistant Professor
University of Pisa
Pisa, Italy

Maurizio Froli, born in 1954, received his Civil Engineering Degree from the University of Pisa where he now teaches Theory of Structures.

Luca SANPAOLESI
Professor
University of Pisa
Pisa, Italy

Luca Sanpaolesi, born in 1927, graduated in Civil Engineering at the University of Pisa. He is Director of the Department of Structural Engineering of the University of Pisa. He is involved in the studies of Eurocodes.

Summary

Fatigue cracks in steel bridges can be prevented by a correct design of the details and by improving execution techniques. The results obtained in the latest research works allow to reduce significantly the risk of occurrence of fatigue cracks in new bridges, but the problem is still open in existing bridges, for which it is necessary to develop suitable repair techniques. In the paper two repair techniques for stiffener to stiffener joints are illustrated and their fatigue behaviour is widely discussed, drawing some relevant conclusion.

1. Introduction

The results obtained in the latest research works concerning the fatigue resistance of orthotropic steel deck bridges [1], [2], [3] allow to improve considerably the fatigue classification as well as the execution techniques of the welded details of this kind of structures.

Of course, the benefits obtained applying the new knowledge are particularly relevant in the design of new bridges, while in existing bridges and also in badly designed new bridges the probability of fatigue crack occurrence in the welded details remains still high. For these reasons, in the last years many research efforts have been devoted to the development of suitable repair techniques for fatigue cracked joints [4].

Being intended to be applied in existing bridges, repair techniques must fulfil some preliminary requirements, in order to minimise the time and the cost required for their execution. On the basis of the aforesaid considerations, a good repair technique should be as simple as possible, avoiding or reducing the traffic flow limitations during the works and assuring a significant residual fatigue life of the repaired details.

In the perspective of the cost reduction and of the maximum efficiency of the repair operation, it is obvious that repairs cannot be limited only to the cracked joints: in fact, to lengthen profitably the time interval between two subsequent repair plans, when fatigue cracks are detected, it is necessary to foresee a complete set of reparations, concerning cracked details as well as similar connections which are fatigue damaged even if not yet cracked.

In the present paper two repair techniques for fatigue cracked stiffener to stiffener welded joints are illustrated and their fatigue resistance, determined by testing real scale specimens, is widely discussed, with particular attention to the comparison between the residual fatigue life of cracked and repaired joints and the fatigue life of the virgin ones.

2. Preliminary results

In the framework of the studies carried out on the virgin connections, the Authors [1], [2] have investigated two types of stiffener to stiffener welded connections, indicated as type I and type II joint in figure 1.

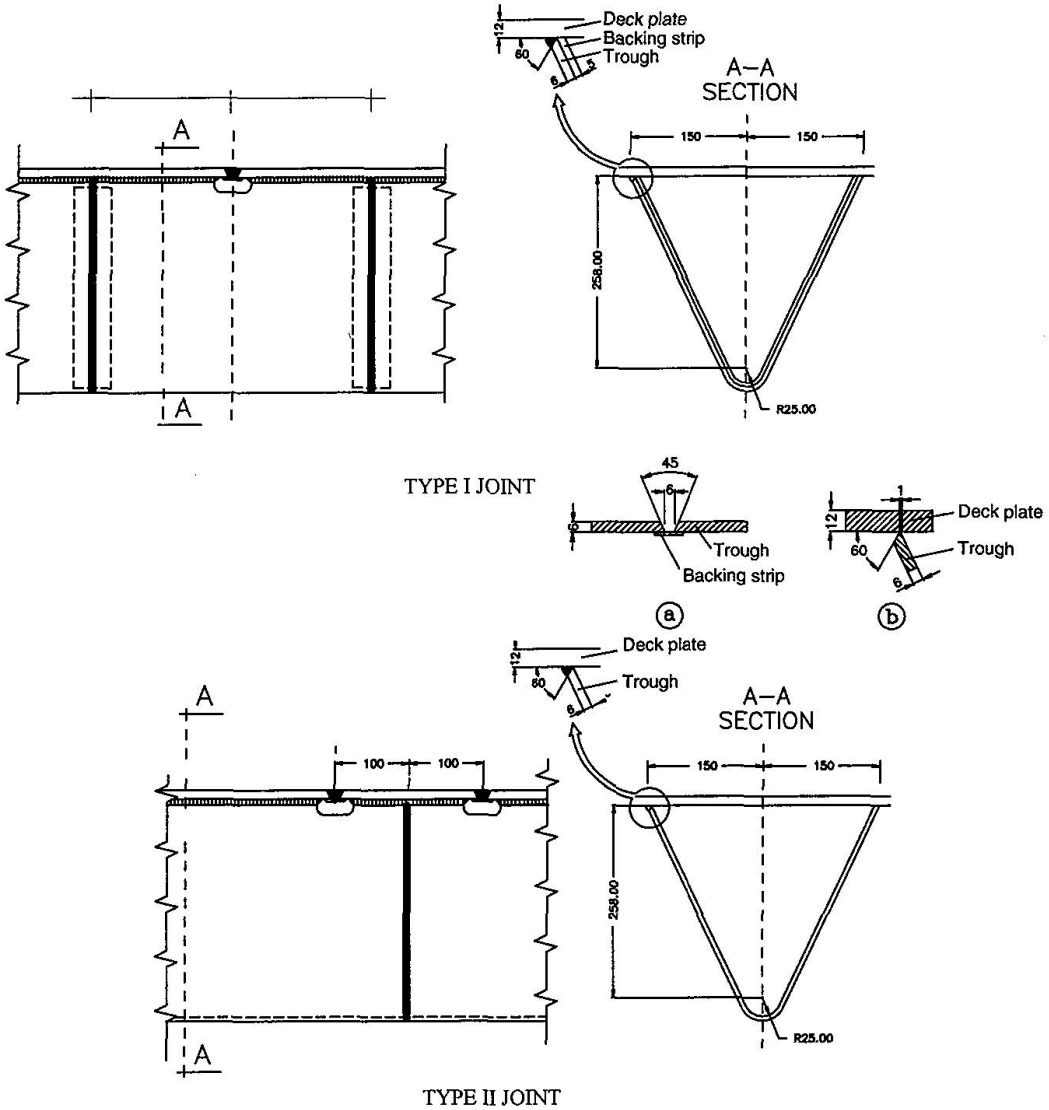

Fig. 1 Stiffener to stiffener connections

The results of constant amplitude fatigue tests, carried out on real scale specimens on a three points bending scheme, are reported in table I and plotted in the S-N diagram of fig.2, in which are reported also the characteristic S-N curves for class 71 and class 80 details of EC3 and the mean S-N curves obtained on tensile specimens with butt welds on backing strip (I* curve) and full penetration welds (II* curve).

Test n.	Connection type	σ_{max} [N/mm^2]	σ_{min} [N/mm^2]	$\Delta\sigma_{max}$ [N/mm^2]	Number of cycles	Remarks
1	I	210	15	195	1390000	-
2	I	240	15	225	539000	-
3	II	240	15	225	251000	-
4	II	210	15	195	939000	-
5	II	190	15	175	821000	-
6	II	190	15	175	459500	-
7	I	240	15	225	468000	-
8	II	155	15	140	6040000	-
9	I	190	15	175	8100000	no crack
10	II	210	15	195	885000	-
11	I	210	15	195	1200000	-
12	I	240	15	225	896000	-
13	II	240	15	225	309000	-
14	II	190	15	175	1930000	-
15	I	210	15	195	1667000	-
16	II	140	15	125	7073000	-
17	I	210	15	195	1622000	-

Table 1 *Fatigue results on stiffener to stiffener real scale virgin joints.*

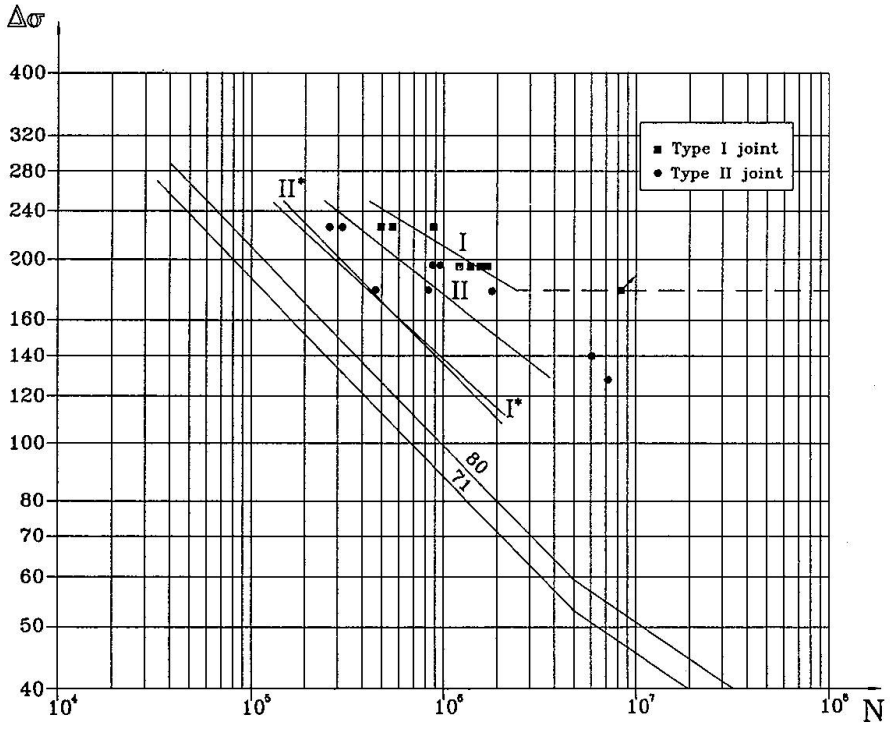

Fig. 2 *Fatigue test results on stiffener to stiffener connections*

3. Repair techniques

Regarding the stiffener to stiffener joints, two different repair techniques, described in detail in the following, have been investigated: the first one, indicated as R1, has been proposed for the rehabilitation of steel bridges in New Zealand [5] and consists in the complete replacement of the cracked joint, while an alternative technique, developed by the Authors and named R2, foresees the use of cover plates.

3.1. R1 repair

The R1 repair of fatigue cracks in stiffener to stiffener connections can be applied to different joint types and requires the following operating sequence leading to a type I joint (fig. 3):

1) Detection of the damaged joints to be repaired.
2) Flame cutting of the damaged part of the stiffener.
3) Preparation of the welding surfaces (according to fig. 3).
4) Backing strips insertion.
5) Fitting of the new stiffener elements and completion, in overhead position, of the welds between the stiffeners and between the stiffeners and the deck plate. (The welders must satisfy the requirements of AWS welder qualification tests for overhead position).
6) Visual, liquid-penetrating and magnetic-particle inspections of the welds and, if necessary, their repair.

3.2. R2 repair

The R2 repair of fatigue cracks, which is especially conceived for strengthening of type I stiffener to stiffener connections (see fig. 1), can be carried out according the following sequence, in such a way that the final geometry shown in fig. 4 is obtained:

1. Determination by means of visual, liquid-penetrating and magnetic-particle inspections of extension and location of the fatigue cracks in the whole joint.
2. Crack milling of the fatigue cracked welds: for the part of the crack located over the backing strip the minimum width of the milling must be equal to 6 mm, namely equal to the former root gap, with a depth of the 6 mm, in order to reach the backing strip (fig. 4); for the part of the crack located out of the backing strip, on the contrary, the result of the milling operation should be an U-groove edge preparation, 6 mm wide and 5 mm deep (fig. 4).
3. Milling of the apex of the fatigue damaged but not yet cracked welds: the minimum width of the milling must be equal to 6 mm, while its depth must be equal to 6 mm in order to reach the backing strip and.
4. Material cleaning and inspection.
5. Execution of the welds in overhead position. (The welders must satisfy the requirements of AWS welder qualification tests for overhead position).
6. Weld grinding in order to set to zero the over-thickness.
7. Visual, liquid-penetrating and magnetic-particle inspections of the welds and, if necessary, their repair.
8. Preparation of the cover plates, 6 mm thick: in the specific case, the dimensions of the cover plate were 1400x185 mm, with a radius of the curved edges equal to 92.5 mm.
9. Execution of fillet welds between the cover plates and the webs of the stiffener. The fillet welds, having a side size of 6 mm, run continuously around the cover plate.
10. Grinding of the fillet welds of the curved edges.
11. Visual, liquid-penetrating and magnetic-particle inspections of fillet welds and, if necessary, their repairs.

When repair concerns fatigue damaged but no-cracked joints, step 2 does not apply.

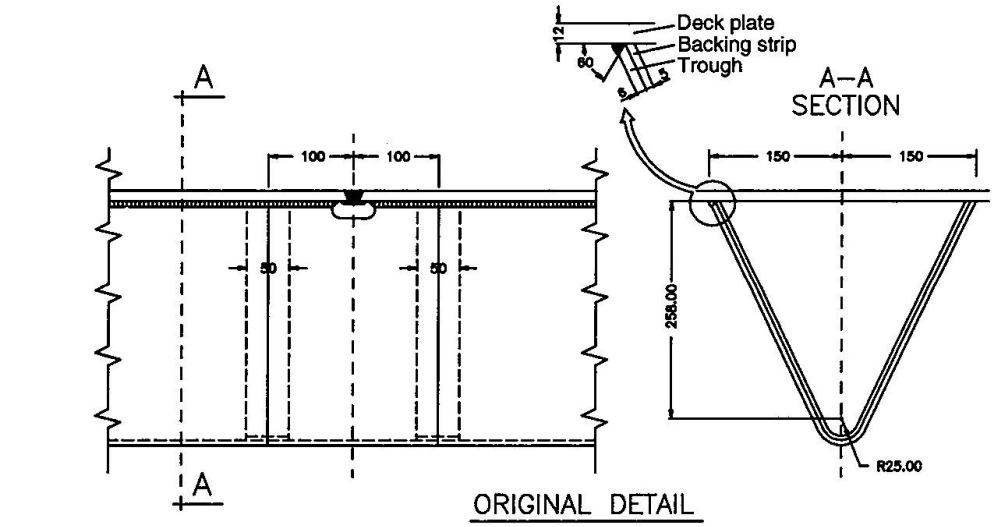

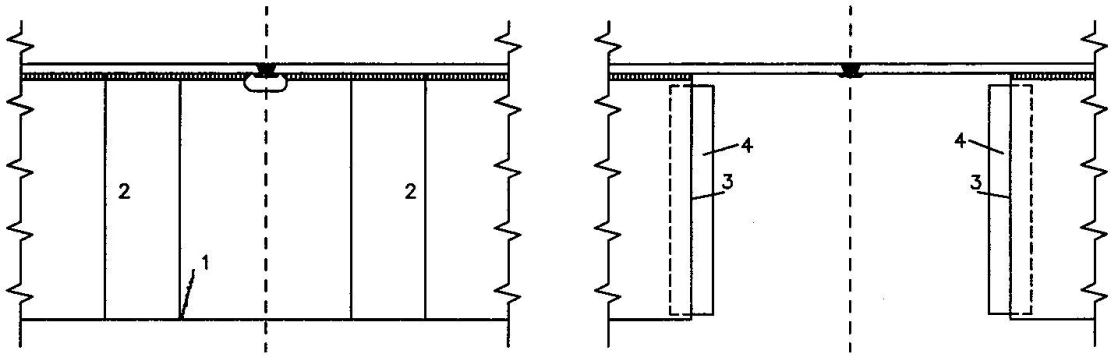

1–Detection of the damaged joint to be repaired;

2–Flame cutting of the damaged part of the stiffener;

3–Preparation of the welding surfaces;

4–Backing strips insertion;

5–fitting of the new stiffener elements and their welding (a and b) together with stiffeners and deck plate.

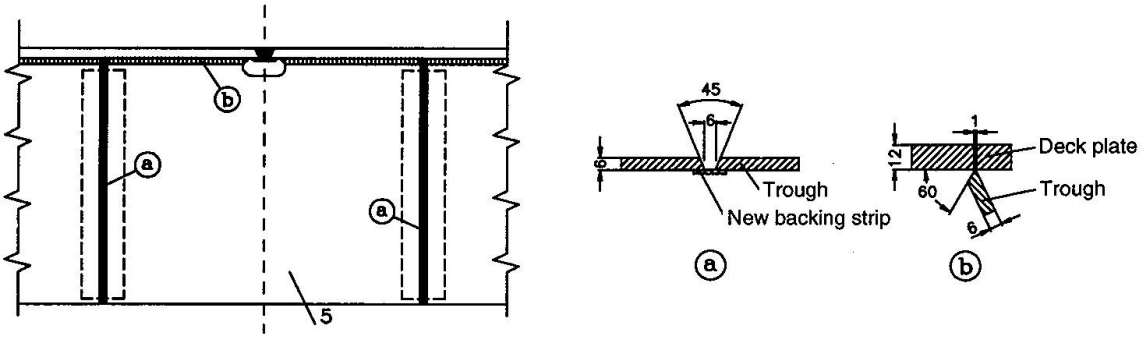

Fig. 3 R1 repair

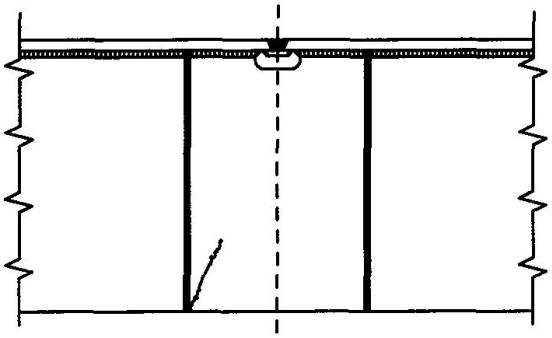

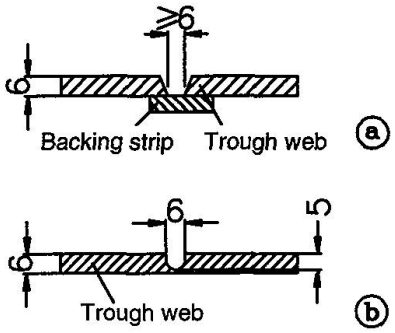

1- Determination of crack extension and location in the whole joint by means of visual, liquid penetrating and magnetic particle inspections.
2- Crack milling. For the part of the crack located over the backing strip the depth of the milling must be equal to 6 mm in order to reach the backing strip; the minimum width must be equal to 6 mm, namely equal to the former root gap (a), while for the part of the crack located out of the backing strip the milling will be carried out in order to obtain an U-groove edge preparation, 6 mm wide and 5 mm deep (b).
3- Milling of the apex of the no-cracked welds.
4- Cleaning and inspections of the material.
5- Executions of the weldings in overhead position. The weldors must satisfy the requirements of the AWS weldor qualification tests for overhead position.
6- Welds grinding to set the over thickness to zero.
7- Visual, liquid penetrating and magnetic-particle inspections of the welds and, if necessary, execution of the repair.
8- Preparation of the coverplates, 6 mm thick. The radius of the curved edges is equal to 92.5 cm while the coverplate dimensions are 1400x185 mm

Trough web

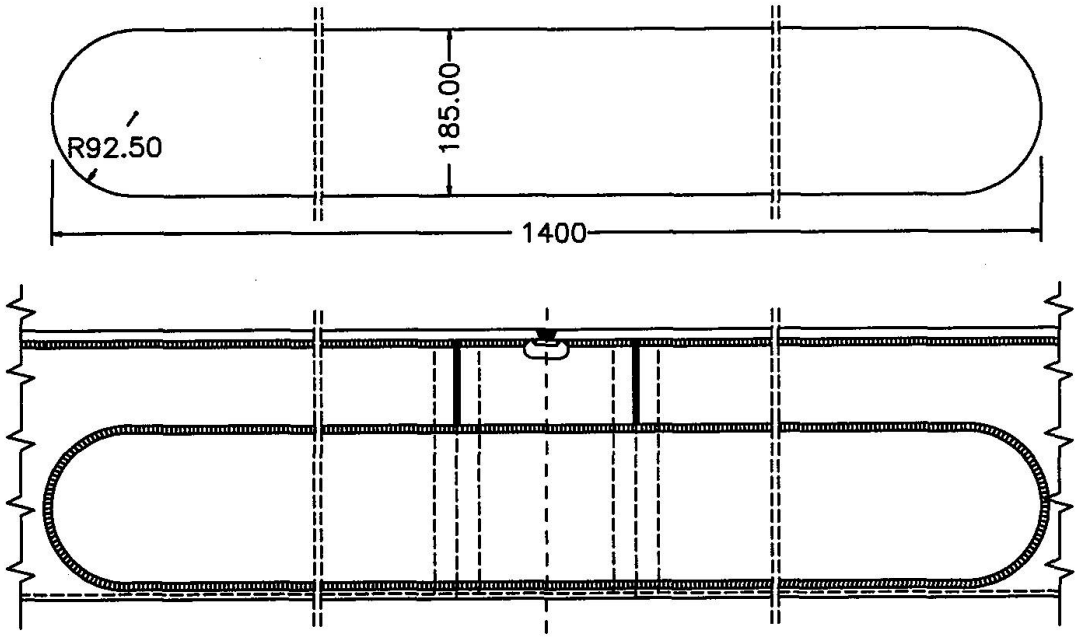

9- Fillet welding of the coverplates to the webs of the stiffener: the fillet side is equal to 6 mm. The fillet runs continuosly around the coverplate.
10-Fillet weld grinding of the curved edges.
11- Visual, liquid penetrating and magnetic-particle inspections of fillet welds and, if necessary, execution of new repairs.

The R2 repair of fatigue damaged but not cracked joints should be performed according the instructions of points 3 to 11.

Fig. 4 R2 repair

3.3. Main features of repair techniques

On basis of the operating sequences described before, it is possible to put in evidence the main features of each repair technique.

In principle, the R1 repair, which seems to be able to restore the original fatigue strength of the joint, can be used for every joint type. It can be applied upon all damaged joints even if not cracked, but during the work it is necessary to deviate the traffic so that the repair operations must be limited, time to time, to small deck areas, increasing the repairing time. Further disadvantages of this technique are related to the difficult fitting of the new stiffener elements to the existing ones and to the possible reduction of the fatigue strength of the deck plate to stiffener joint.

The R2 repair can also be carried out both on cracked and uncracked joints but it seems, at first sight, unable to restore the original fatigue strength of the joint, because the damaged areas are not completely removed. Nevertheless it must be noted that, locally, the section modulus of the stiffener becomes higher, due to the effect of the cover plates, so that the stress level in the weld, at the apex of the stiffener, is considerably reduced. On the base of these considerations, the additional fatigue life could be relevant. Besides, the R2 repair appears easier, cheaper and quicker in execution than the R1 repair, even if its application is limited to type I joints.

4. Fatigue tests on repaired specimens

In order to evaluate the additional fatigue life of the repaired connections, to be compared with the fatigue life of virgin ones and with the expected residual life of the orthotropic deck, test specimens in real scale have been prepared, reproducing the effective field situation, using the fatigue cracked specimens obtained from the previous research [1], [2]: taking into account the peculiarities of each type of repair, type I joints have been repaired using the R2 technique, while type II joints have been repaired using the R1 technique.

Constant amplitude fatigue tests on repaired stiffener to stiffener connections have been carried out on a three points bending scheme, with the pulsating load on the joint axis, located at the mid-span of the stiffener (Figure 5).

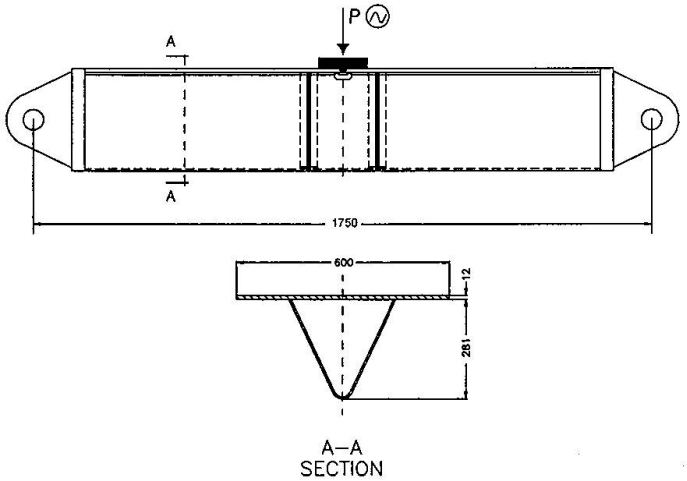

Fig. 5 Fatigue test scheme for repaired stiffener to stiffener connections

The fatigue test results are reported in table 2 and in the S-N diagram of figure 6, in which are also reported the characteristic S-N curves for class 71 and 80 details of EC3 and the relevant mean S-N curves already shown in fig. 1.

The test results on R2 repairs are reported in terms of nominal stresses, both taking into account the section modulus increase due to the presence of the cover plates (these stresses are indicated as *actual stresses)* or not, i.e. considering the stresses which should be obtained in the original cross section, disregarding the presence of the cover plates themselves. Obviously, for R1 repaired specimens are considered only nominal stresses.

N.	Type of repair	σ_{actmin} [N/mm²]	σ_{actmax} [N/mm²]	$\Delta\sigma_{actual}$ [N/mm²]	$\Delta\sigma_{nominal}$ [N/mm²]	Number of cycles
1	R2	15	180	165	250	250 000
2	R1	15	240	225	225	875 000
3	R1	15	240	225	225	750 000
4	R2	15	151	136	200	1 650 000
5	R2	15	89	74	109	2 560 000
6	R1	15	240	225	225	700 000
7	R2	15	166	151	230	2 850 000
8	R1	15	240	225	225	60 000
9	R1	15	185	170	170	190 000
10	R2	15	166	151	230	450 000
11	R1	15	185	170	170	310 000
12	R1	15	130	115	115	750 000
13	R1	15	130	115	115	1 200 000

Table 2 *Test results on stiffener to stiffener repaired joints*

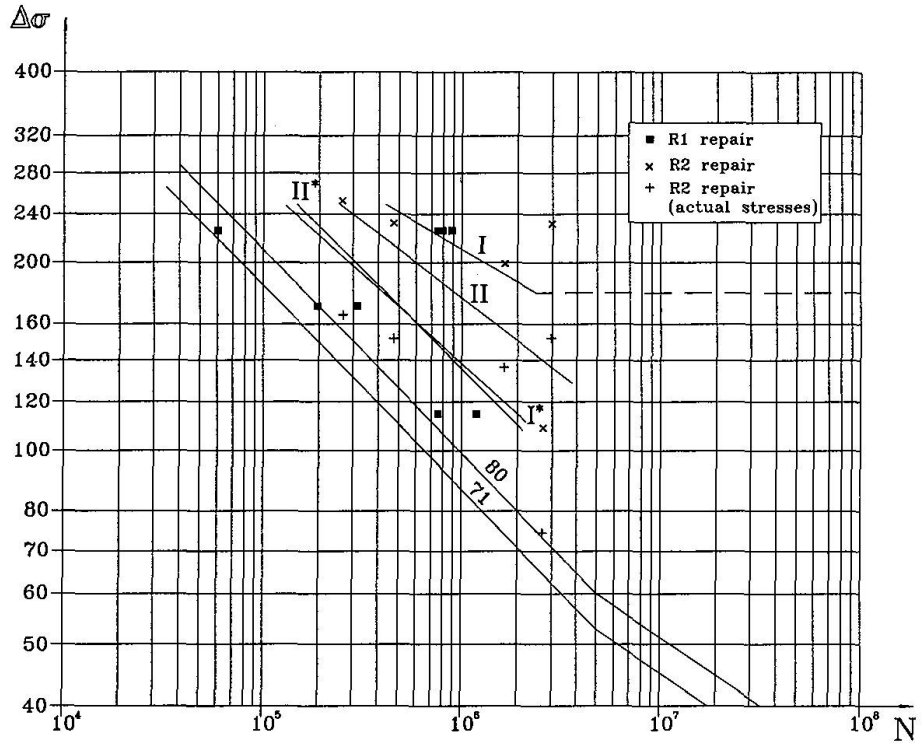

Fig. 6 *Fatigue test results on repaired stiffener to stiffener connections*

Concerning the failure mode, it has been observed that in R1 repaired specimens cracks start always at the apex of the stiffener, in the weld, propagating in the weld itself; while in R2 repaired specimens n.1 and n. 10 cracks start at the apex of the stiffener, in the weld, propagating through the cover plates, and in R2 specimens n. 4, n. 5 and n. 6 the cracks start at the apex of the stiffener in correspondence of the tack weld of the baking strip, propagating through the cover plates.

The test results show that :

- the fatigue strength is more scattered for repaired joints than for virgin ones;
- all test results are above the characteristic S-N curve for class EC3 71 detail;
- the original fatigue life is not completely restored with R1 repair;
- R2 repair gives, in terms of actual stresses, the same residual fatigue life as R1 repair;
- in terms of nominal stresses, i.e. with the same traffic loads, R2 repair gives a residual life appreciably higher than that assured by R1 repair and comparable with the fatigue life of type II virgin joints;
- R1 repair can be classified as 71;
- R2 repair can be classified as 71, in terms of actual stress;
- R2 repair can be classified as 100, in terms of nominal stress.

5. Conclusions

The fatigue tests carried out on repaired specimens lead to the following relevant conclusions about the two repair techniques, which have been proposed for stiffener to stiffener joints, even in view of design recommendations :

1) both techniques can be easily performed;
2) fatigue behaviour of the R2 repair is not significantly influenced by the welding of the cover plate;
3) the original fatigue life is not completely restored with R1 repair;
4) R2 repair gives a residual life appreciably higher than that assured by R1 repair and comparable with the fatigue life of type II virgin joints;
5) R1 repair can be classified as 71;
6) R2 repair can be classified as 100, in terms of nominal stress;
7) R2 repair technique almost restores the fatigue life of the joint and it represents a good compromise between costs and benefits, so that it results suitable for practical applications.

References

1. CARAMELLI, S.; CROCE, P.; FROLI, M.; SANPAOLESI L.: Fatigue Behaviour of Orthotropic Steel Bridge Decks, IABSE Workshop on Remaining Fatigue Life of Steel Structures, Lausanne, 1990, pp. 271-280.
2. CARAMELLI, S.; CROCE, P.; FROLI, M.; SANPAOLESI L.: Fatigue Behaviour of Steel Decks of Cable Stayed Bridges. Proceedings of 1994 International Symposium & Exhibition on Cable Stayed Bridges, Shanghai, 1994.
3. BRULS, A.; BEALES, C.; BIGNONNET, A.; CARAMELLI, S.; CROCE, P.; FROLI, M.; JACOB, B.; KOLSTEIN, M. H.; LEHRKE, H.; POLEUR, E.; SANPAOLESI, L.: Measurement and interpretation of dynamic loads in bridges - Phase 3: Fatigue behaviour of orthotropic steel decks, Technical Steel Research. Synthesis report EUR 13378 EN, Commission of the European Communities, Luxembourg, 1991.
4. BRULS, A.; BEALES, C.; CARAMELLI, S.; CARRACILLI, J.; CUNUNGHAME, J.,; CROCE, P.; FROLI, M.; KOLSTEIN, M. H.; LEENDERTZ, J. S..; LEHRKE, H.; LE PAUTREMAT, E.; SANPAOLESI, L.: Measurement and interpretation of dynamic loads in bridges - Phase 4: Fatigue strength of steel bridges, Technical Steel Research. Synthesis report, Commission of the European Communities, Luxembourg, 1996.
5. ALLAN, J.D.; POLKINGHORNE, N.; WEIN, K.: The repair of fatigue cracked joints in the orthotropic deck stiffeners of the Auckland Harbour Bridge, New Zealand Institute of Welding Conference, 1987.

Leere Seite
Blank page
Page vide

Fatigue Test of a Large Diameter Steel Wire Rope of a Cable-Stayed Bridge

Onno D. DIJKSTRA
Civil Engineer
TNO
Rijswijk The Netherlands

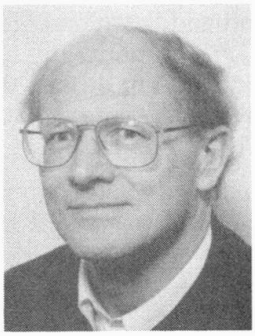

Onno Dijkstra, born 1945, received his civil engineering degree at the Delft University of Technology. Since 1974 he has worked for TNO and has been involved in fatigue and fracture mechanics research and consulting.

Frank van DOOREN
Senior Engineer
Dir.-Gen. Public Works
Zoetermeer, The Netherlands

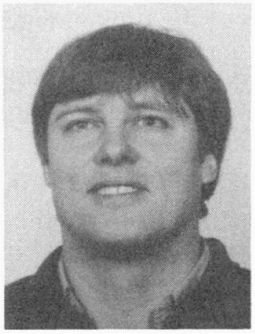

Frank van Dooren, born 1963, received his civil engineering degree at the Delft University of Technology. Since 1988 he has worked for the Directorate - General for Public Works and Water Management and is now senior engineer at the steel department of the Civil Engineering Division.

Summary

Broken wires were found in the cables of a bridge after 15 years in service and it was decided to fatigue test a spare length of the cable. This paper presents the results of the fatigue test on a large diameter (∅ 101 mm) locked coil cable of the bridge. The initial variable amplitude fatigue load was determined by measurements on the bridge. A high constant amplitude fatigue load was necessary to get wire failures in the cable. The test shows that the cable is capable of resisting the design load although deterioration of the cable is clearly visible on the outside of the cable. Based upon the results it was recommended not to take any replacement actions. Monitoring the cables every five years was recommended.

1. Introduction

During maintenance work of the locked coil cables (∅ 101 mm) of a cable stayed bridge some broken wires were found. At that time the bridge was 15 years in service. The management of the bridge was concerned about the remaining lifetime of the cables.

Preliminary investigations of the fracture surface of some broken wires removed from the bridge cables indicated that fatigue starting from minor fabrication defects were the cause of the wire failures. These defects were laps, defined as imperfections caused by impressing or working an excess of metal or an irregularity into the surface of a wire.

At the time of bridge erection a 4 meter cable with conical end sockets was supplied and placed on the bridge. This was available for testing and was transported to the laboratories of TNO Building and Construction Research in Rijswijk, Netherlands and tested in a 10 MN test rig.

The cable was installed and prestressed before fatigue testing. The fatigue test was carried out in three phases with three different increasing load spectra. After the fatigue test the cable was dismantled into separate wires. The experimental results were evaluated and fatigue fracture mechanics analyses were carried out on single wires [1], thus enabling conclusions with regard to the remaining fatigue life to be made.

2. Preliminary investigations

After the "lucky" discovery of some broken wires in the cables of the bridge, the total length was investigated during maintenance work. The widths of openings in broken wires were measured. The relatively small number of broken wires and the small width of openings due to cracks (reduction of cable cross-sectional area only over a short length) indicated that there was no immediate danger for the use of the bridge.

Parts of the broken wires were taken out for investigation and the actual effect of the traffic (stress spectrum during an ordinary day) was measured. Preliminary fatigue analyses indicated that the laps found on the broken wires were too small to result in broken wires after such a short time. However, no other explanation than fatigue initiated at the laps due to the traffic load could be found.

Because the inside of the cables could not be investigated easily and no simple model could be made to investigate the future deterioration of the cables TNO was asked to carry out a fatigue test on the available 4 meter cable with sockets.

3. Test specimen and instrumentation

The specimen is a locked coil cable with both ends provided with end sockets. The free cable length between the sockets is 3.72 m. The cable has 9 layers of wires. The outer two layers were full lock Z shaped wires (see Figure 1). Further specifications were as follows:

Nominal diameter	D	= 101 mm
Cross-sectional area	A	= 6900 mm^2
Minimum breaking load	Ff	= 9030 kN
Aggregate breaking load	Fa	= 10076 kN
Apparent Young's modulus	Ea	= 150000 N/mm^2

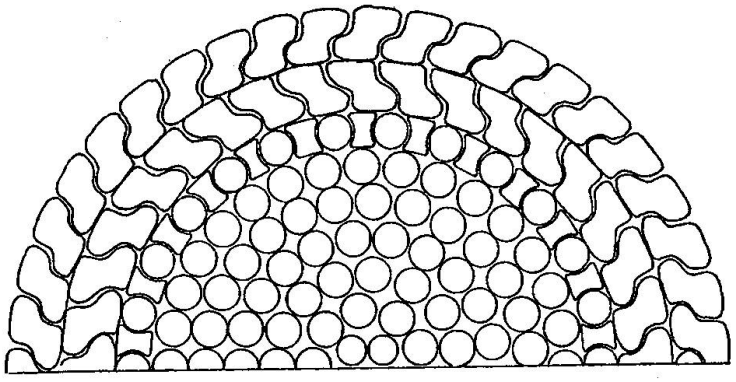

Fig. 1 Cross-section of steel wire rope

The specimen was equipped with ten strain gauges on the outer wires. These gauges were located on different wires in two cross-sections at 1/3 and 2/3 of the cable length. Displacement measurements between the two sockets were carried out during the whole test. Displacement of the socket filler material was measured during the second part of the fatigue test as it turned out that the socket filler material was moving into the sockets.

4. Loading

4.1 Preloading

Before the fatigue test the cable was preloaded. This was done in the same way as for the cables in the bridge. The cable was loaded ten times between 900 kN and 3000 kN. Strain and deflection measurements were carried out during preloading. From these measurements an apparent Young's modulus of 156000 N/mm^2 was found (nominal value 150000 N/mm^2). The measured strain range corresponds very well with the theoretical value (based on cross-sectional area and Young's modulus equal to 210000 N/mm^2).

4.2 Fatigue testing

The fatigue loading on the cable during the first phase was based on strain measurements on the cables in the bridge in the year 1990 during 11 hours. Using traffic counting during a longer period the measurements were extrapolated to a year spectrum of 817898 cycles. The cumulative year spectrum of the stress ranges is given in Figure 2.

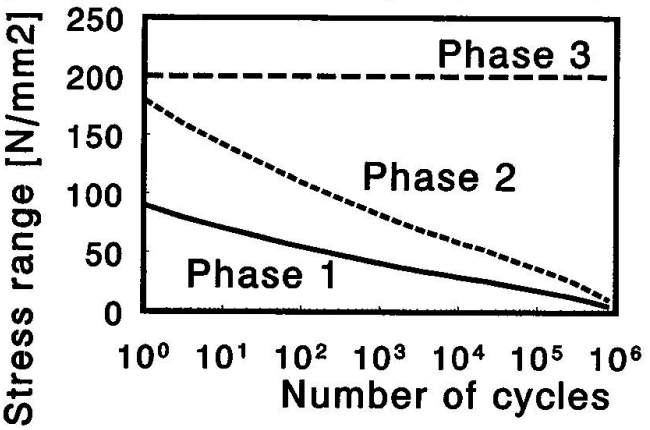

Fig. 2 Cumulative stress spectra

Using a random selection procedure the stress ranges of the year spectrum were put in a certain sequence and translated to a variable load sequence for the cable. The minimum loads were set at a constant value of 2350 kN (stress in the cable 341 N/mm^2), corresponding to the dead weight load in the cable in the bridge. With a maximum stress range of 90 N/mm^2 in the spectrum the maximum load in the cable is 2971 kN. The maximum load range is approximately 70 % of the load range due to the design traffic load.

The frequency of the loading was depending on the magnitude of the load(stress) range according to Equation (1), with a maximum frequency of 5 Hz, giving an average frequency of 4.16 Hz.

$$f = 53 / \Delta\sigma \qquad (1)$$

A total of 30 million cycles (approximately 37.7 year spectra) were applied to the specimen. As no visible or measured damage was noticed the fatigue test was stopped and the test was continued with a higher fatigue load in the second phase.

In the second phase the variable part of the loading was doubled with regard to the first phase (see Figure 2). The minimum load was kept on the first phase level (2350 kN). The same relation between load range and frequency was used, resulting in an average frequency of 2.5 Hz for the second phase. The maximum load during the second phase was 3592 kN.

A total of 4 million cycles (approximately 4.9 year spectra with double stress ranges) were applied to the specimen. As again no visible or measured damage was noticed the second phase of the fatigue test was stopped and the test was followed by the third phase.

In the third phase a constant amplitude load with a load range of 1380 kN ($\Delta\sigma$ = 200 N/mm^2) was applied (see Figure 2). The minimum load was again 2350 kN. The frequency in the third phase was 0.45 Hz. The maximum load during the third phase was 3730 kN.

A total of 1.266 million cycles were applied to the specimen in this third phase.

5. Experimental results

5.1 Phase 1 and 2

During phase 1 and 2 the regular measurements of the displacements and the strains did not show very interesting results.

The only real interesting thing is that the socket filler material was moving into the conical socket. This was discovered during the first phase after approximately 3 million cycles. From then on this phenomenon was measured by a displacement gauge at the centre of the back of the conical socket. This movement of the socket filler material results in an increase in the distance between the sockets. So, the displacement gauges for the change in length of the cable are also measuring this movement.

5.2 Phase 3

During this phase a small number of wires were broken and a larger number of wires were pulled out from the sockets. Most of the failed wires were from the outer layer (layer number 9). The development of the number of broken or pulled-out wires of the outer layer is almost linearly proportional to the number of cycles (see Figure 3). The first wires to be pulled out (two) were found after 463000 cycles and at the end of the test at 1.266 million cycles a total of 32 outer wires were broken or pulled-out.

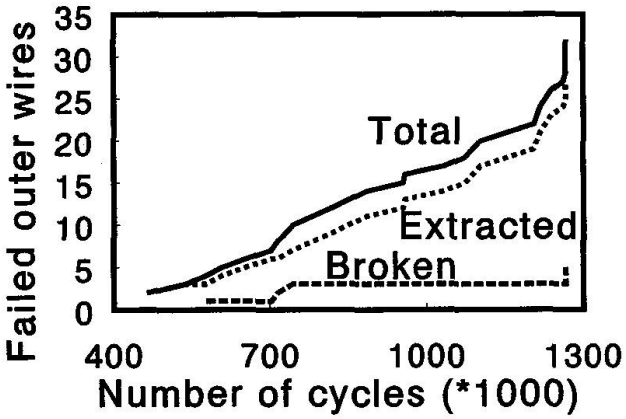

Fig. 3 Number of broken or pulled-out outer wires as a function of the number of cycles

After the test the cable was unravelled and seven additional broken or pulled-out wires were found in internal layers (4 in layer 8 and 3 in layer 7).

The test was load controlled, so that broken wires resulted in an increase in displacements.

Recordings of the strain and displacement gauges were carried out 52 times during the 1.266 million cycles. Measurements were taken at the minimum value of the load cycle (2350 kN) and the maximum of the load cycle (3730 kN).

The recording of the change in distance between sockets as the test load cycled from the minimum to the maximum load indicated an increase in flexibility at the end of the test due to broken and pulled-out wires (see Figure 4). The theoretical change in length due to the loss of cable section is approximately 5 mm. This agrees well with the measured value of between 4.5 and 5.0 mm.

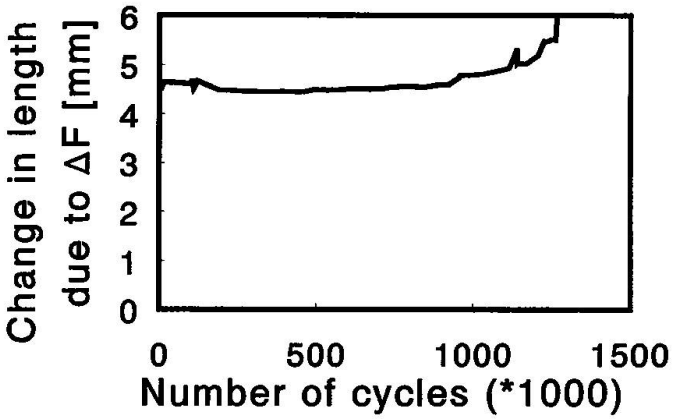

Fig. 4 Change in length due to load range as a function of the number of cycles

The loss in cross-section due to broken wires at the end of the test was approximately 20%. This means an increase in flexibility of 25%. The change in length at the end of the test was approximately 6 mm. These figures agree very well with each other.

The increase in distance between the sockets at maximum load during the fatigue test is approximately 22 mm (see Figure 5). The displacement of the socket filler material is responsible for 5 mm of this displacement (see Figure 6). The loss of 32 outer wires means a loss in cross-section of 1650 mm^2 (6900 mm^2 to 5250 mm^2) and can be equated to an additional length at maximum load of 4 mm. The loss of the wires in the inner layers (7 broken wires) is responsible for 1 mm. The remaining increase in length of 12 mm can not be explained directly. Causes for this length increase can be an overall sliding of the wires in the socket filler material or relatively more sliding of the inner wires with regard to the outer wires.

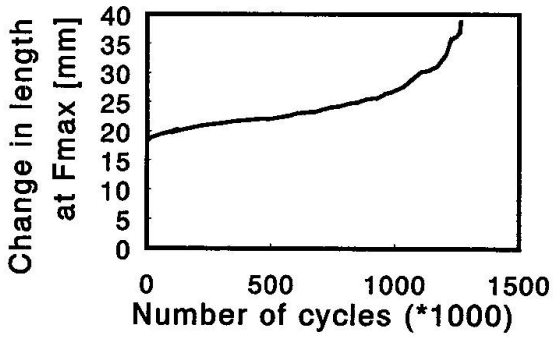

Fig. 5 Increase in length at maximum load as a function of the number of cycles

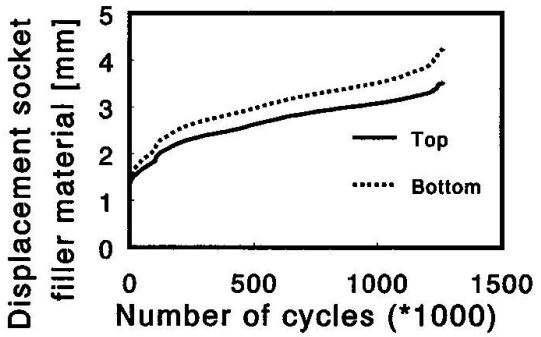

Fig. 6 Displacement of socket filler material as a function of the number of cycles

The strain measurements on the ten wires gave a clear indication of when a wire was broken or pulled out. In some cases it turned out that the strain readings gave an indication before the failure was discovered by visual inspection.

In some cases there seems to be an inconsistency between the readings of the strain range and the maximum strain. However it is likely that a broken wire is still strained by the fluctuating load (due to support of the neighbouring wires) while the maximum (or average) strain has dropped due to the failure.

6. Fracture and wire surface analyses

After the fatigue test the wires of the specimen were unravelled. The results of this unravelling can be summarised as follows (layer numbering from inside to outside):

layer 1 to 6	- no failures
layer 7	- 3 broken wires in the free length (1x round and 2x half lock)
layer 8	- 4 broken wires in the free length
layer 9 (outside)	- 32 failed wires, of which:

. 13 pulled out from the top socket
. 1 broken in the top socket
. 5 broken in the free length
. 7 broken in the bottom socket
. 6 pulled out from the bottom socket

Fracture analyses were carried out on 13 fracture surfaces. Nine of the failures were due to fatigue initiation from laps. Three failures showed no fatigue crack growth and were caused by overloading. One wire failed due to the presence of an unexplained severe mechanical defect.

Wire surface inspections were carried out on 12 wires. Some of the wires were chosen randomly and others were from broken wires. The random wires showed no defects, minor longitudinal grooves or a light crackle pattern. A number of the broken wires showed laps on the surface and a maximum lap depth of 0.5 mm was found.

7. Evaluation

7.1 General

The translation of the behaviour of the test specimen to the behaviour of the cables in the bridge is not simple. The main reasons for the difficulties are:

- The difference in length of the specimen (≅ 4 m) and the length of the cables in the bridge (≅ 6000 m). Applying the weakest link model to this situation means that we can consider the cable in the bridge as 1500 test specimens. The question is: "What is the relation between the test specimen and the weakest link in the cable".
- The fatigue load in the test is different from the fatigue load on the bridge cable (only for phase 2 and 3).
- At the end of the fatigue test the specimen was not failed completely. The maximum load in the fatigue test (3730 kN) could still be applied to the specimen, while the maximum design load (only 3250 kN) is below this value. The theoretical breaking load of the cable is 9000 kN.

In the next sections evaluations are made using the results of the total specimen (Miner summations and statistical evaluations) and fatigue fracture mechanics analyses of single wires.

7.2 Total rope evaluation

7.2.1 Cumulative damage evaluation

Using the Palmgren-Miner cumulative damage rule (Equation (2)) the total damage of the three different load spectra can be determined.

$$D_{tot} = \sum_i D_i = \sum_i \frac{n_i}{N_i} \tag{2}$$

where:
D_{tot} = total cumulative damage
D_i = cumulative damage due to stress range $\Delta\sigma_i$
n_i = number of stress ranges $\Delta\sigma_i$
N_i = lifetime at stress range $\Delta\sigma_i$

For the $\Delta\sigma$-N curve a conservative straight curve can be used (Equation (3))

$$(\Delta\sigma)^m \cdot N = (\Delta\sigma_{ref})^m \cdot N_{ref} = C \tag{3}$$

where: m = slope $\Delta\sigma$-N curve
C = a constant determining the level of the $\Delta\sigma$-N curve

Combining the two equations above gives the ratio (R_{Dexp}) between the damage of an experimental spectrum (D_{exp}) and the damage of the year spectrum ($D_{j\text{-}sp}$)

$$R_{D\exp} = \frac{D_{\exp}}{D_{j-sp}} = \left(\frac{\Delta\sigma_{\exp}}{\Delta\sigma_{j-sp}}\right)^m \cdot \frac{n_{\exp}}{n_{j-sp}} \tag{4}$$

Equation (4) can be used with an equivalent stress range ($\Delta\sigma_{eq}$) for the spectrum according to Equation (5).

$$\Delta\sigma_{eq} = \left[\frac{\sum_i \left(\Delta\sigma_i^{\,m} \cdot n_i\right)}{\sum_i n_i}\right]^{\frac{1}{m}} \tag{5}$$

The value for the slope of the S-N curve (m) is dependent on the ratio of the total life and the crack growth life. A conservative value for crack growth only is $m = 3$. For the wires of the cable a more realistic value will be 4 or 5. The calculated values for the equivalent stress range ($\Delta\sigma_{eq}$) is as follows:

13.6 N/mm^2 for $m = 3$
15.2 N/mm^2 for $m = 4$
17.0 N/mm^2 for $m = 5$

The damage of phase 3 is governing in the damage analysis (see Table 1). The damage is very much depending on the value of m. Without further information a value of 4 is considered as conservative. This conservative value gives an experimental damage equivalent to the 46000 year spectra.

Loading	Slope S-N curve m	Stress ratio $R\sigma = \Delta\sigma_{exp} / \Delta\sigma_{j\text{-}sp}$	Stress correction factor $f\sigma = R\sigma^m$	Lifetime correction factor $fn = n_{exp} / n_{j\text{-}sp}$	Relative damage $R_{Dexp} = f\sigma * fn = D_{exp} / D_{j\text{-}sp}$
phase 1	3 , 4 or 5	1	1	36.7	36.7
phase 2	3	2	8	4.89	39.1
	4	2	16	4.89	78.2
	5	2	32	4.89	156.5
phase 3	3	14.7	3189	1.55	4937
	4	13.1	29614	1.55	45841
	5	11.8	225375	1.55	349331
Total damage for phase 1+2+3	3				5013
	4				45956
	5				349524

Table 1 *Damage analysis according to Palmgren-Miner*

7.2.2 Statistical evaluation

Without further knowledge one test result is not enough to make a statistical evaluation (no information about scatter). However, using existing knowledge about the behaviour of welded steel specimens one can make a statistical analysis.

The standard deviation for welded joints using a lognormal distribution is approximately a factor of 1.5 on lifetime (standard deviation is ln(1.5) on the logarithmic scale)[2]. The slope of the $\Delta\sigma$-N curve is 3 for welded joints. It is generally known that for specimens smoother than welded specimens the slope and the scatter is higher. The wires of the cable can be considered as smooth specimens. Therefore the factor for the scatter has to be increased for larger values of m.

A design line is generally the mean minus two standard deviations. This means that with the slope of 3 and the factor of 1.5 on life there is a ratio of 2.25 for the level of the mean line and the design line. It is assumed that for the slopes of 4 and 5 this ratio will be doubled, so:

slope	ratio mean/design f^2	standard deviation on logarithmic scale ln(f)
3	2.25	ln(1.500)
4	4.50	ln(2.121)
5	9.00	ln(3.000)

The experimental result as evaluated in the section above has to be considered as the average value. Due to the fact that we have only one experimental result the standard deviation has to be increased with a factor F_0 depending on the number of specimens n (here $n = 1$).

$$F_0 = \sqrt{1+\frac{1}{n}} \qquad \text{so:} \quad F_0 = \sqrt{2} \tag{6}$$

So, the relative design damage ($R_{Ddesign}$) can be determined as follows:

$$\ln(R_{Ddesign}) = \ln(R_{D\exp}) - 2\cdot\sqrt{2}\cdot\ln(f) \quad \text{or} \quad R_{Ddesign} = R_{D\exp}\cdot f^{-2\cdot\sqrt{2}} \tag{7}$$

The calculated relative design damage ($R_{Ddesign}$) is well above a relative design damage in 75 years ($R_{D75} = 75$) (see Table 2).

Assuming end of test as failure the reliability index (β) and the failure probability (Pf_{4m}) for the specimen with a length of approximately 4 m can be determined with Equation (8)

$$\beta = \frac{\ln(R_{D\exp}) - \ln(R_{D75})}{\sqrt{2}\cdot\ln(f)} \tag{8}$$

The failure probability of the cable in the bridge (length 6 km) can be determined by multiplying Pf_{4m} with 1500 (= 6000 / 4). The calculated failure probabilities (see table 2) increase with increasing slope (value of m). The more favourable mean lives for higher values of m are override by the higher assumed scatter. The calculated failure probabilities are low with regard to normal design requirements ($Pf = 1.6*10^{-4}$).

Slope S-N curve m	Relative damage experiment R_{Dexp}	Relative design damage $R_{Ddesign}$	Reliability index β	Failure probability 4 m cable Pf_{4m}	Failure probability 6 km cable Pf_{6km}
3	5013	1592	7.329	$1.2*10^{-13}$	$1.8*10^{-10}$
4	45956	5477	6.034	$8.3*10^{-10}$	$1.2*10^{-6}$
5	349524	15631	5.437	$2.8*10^{-8}$	$4.2*10^{-5}$

Table 2 *Relative design damage, reliability index and failure probability for 75 years*

7.3 Crack growth analyses

A fracture mechanics crack growth analysis was carried out on the single wire geometry. In these analyses the initiation phase is neglected and only the lifetime from an initial defect to a final defect is determined. The Z-shaped wire is schematised to a square cross-section with a length of 7 mm and a constant depth edge crack at one side. The stress intensity factor used was for membrane stress only and for a bending restrained situation [3]. It is assumed that the wire is supported by the neighbouring wires so that no bending deformation can occur.

The crack growth parameters for an average and for a design (safe) *da/dN-ΔK* curve are taken from PD 6493 [4]. A range of initial defects was used (from 0.1 mm to 1.0 mm). The final defect for all analyses was 4 mm. The equivalent stress ranges of the bridge spectrum mentioned earlier are used.

The results of the crack growth analyses expressed as the lifetime in years, carried out with the TNO program FAFRAM [5], are given in Table 3. It should be pointed out that for small cracks the stress intensity factor is very low and well below the threshold value for normal steel. So it can be expected that the values in Table 3 are very conservative. The lowest design life is 74 years for a stress range of 17.0 N.mm^2 and an initial defect of 1.0 mm. The lifetimes determined for small initial defects are of the same order of magnitude as those found in Section 7.2.2 for $m = 3$.

Initial defect	Stress range 13.6 N/mm^2		Stress range 15.3 N/mm^2		Stress range 17.0 N/mm^2	
[mm]	$L_{average}$	L_{design}	$L_{average}$	L_{design}	$L_{average}$	L_{design}
0.1	1645	1004	1155	705	842	514
0.2	1026	626	720	440	525	321
0.3	756	461	531	324	387	236
0.4	597	365	419	256	306	187
0.5	490	299	344	210	251	153
0.6	413	252	290	177	211	129
0.7	354	216	248	152	181	111
0.8	307	187	216	132	157	96
0.9	269	164	189	115	138	84
1.0	237	145	166	102	121	74

Table 3 *Lifetime in years according to fatigue fracture mechanics analyses*

8. Conclusions, remarks and recommendations

The direct conclusions based on the evaluation of the experimental results are as follows:

- Most of the wire failures were fatigue cracks initiated at laps on the full lock wires.
- An evaluation based on Miners rule and a statistical analysis (using existing general fatigue knowledge) gives design lives of 1000 year or higher and a probability of failure for the cables in the bridge of $4*10^{-5}$ or lower.
- Fracture mechanics crack growth analyses on single wires showed design lives ranging from 75 to 1000 years.
- The general behaviour of the cable during the fatigue test showed that the degradation process is gradual. At the end of the fatigue test with a number of failed wires the cable was still capable to carry a load higher than the maximum design load.

For the bridge management the test has provided a better understanding of the fatigue behaviour of the cable and the evaluation of the test results showed an adequate safety of the cables during the design life of the bridge.

The experiment showed further that the problems are confined to the full locked wires in the outer layer. This combined with the fact that the width of openings at cracks in the broken wires

of the bridge remains small (reduction of cross sectional area only over a short length) leads to the conclusion that the remaining area in any cross section will stay large even though a number of wires were broken over the length of the cables.

The experiment shows that the specimen is capable of resisting more than the design load although deterioration of the cable is clearly visible on the outside. So, the system warns before failure.

Based upon the results the bridge management was recommended not to take any replacement actions. It was recommended to monitor the actual state of the cables every five years.

References

1. DIJKSTRA, O. D., "Cable for bridge", TNO report 96-CON-R0527 (in Dutch).

2. British Standard Institution "Steel, concrete and composite bridges ; Part 10. Code of practice for fatigue" BS 5400 : Part 10 : 1980.

3. HARRIS, D. O. , J. Bas. Engineering, 89 (1967), p. 49.

4. British Standard Institution "Guidance on methods for assessing the acceptability of flaws in fusion welded structures", PD 6493 : 1991

5. DIJKSTRA, O. D., and STRAALEN, IJ. J. van, "Fatigue crack growth program FAFRAM (FAtigue FRActure Mechanics)" TNO report BI-91--51

Fatigue Strength of Riveted Connections

Geoffrey L. Kulak
Professor
University of Alberta
Edmonton, AB, Canada

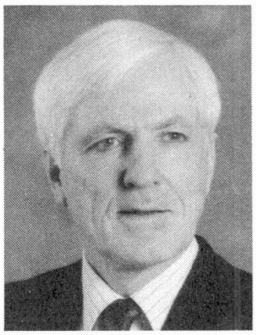

Geoffrey Kulak received engineering degrees from the University of Alberta, University of Illinois, and Lehigh University. He has been Professor of Civil Engineering at the University of Alberta, Edmonton, since 1970 .

Summary

The fatigue life behavior of riveted members is a matter of considerable interest, even though new riveted structures have not been built in the past several decades. The life of the large stock of riveted bridges that still exist must be extended, while at the same time maintaining a safe condition. Test results on full-size flexural members and axially loaded members are reported. These test results are compared with the design recommendations of several European and North American standards. Recommendations are presented for a fatigue life classification.

1. Introduction

Because new riveted structures have not generally been built in the past several decades, less attention has been paid to their fatigue strength behavior than to structures containing contemporary fastening elements such as bolts or welds. The behavior of riveted members is a matter of considerable importance to owners and regulatory authorities, however. Evaluation of the remaining fatigue life of a riveted structure has been impeded by the lack of a reasonable data base of test results of full-size members. However, recent work in both North America and Europe has addressed this need for better fatigue strength data for this category . Although more data are always welcome, the data base is now sufficiently large to be able to present the foundations for fatigue strength evaluation of riveted members with reasonable confidence.

2. Determination of Fatigue Life

2.1 Basis of Fatigue Strength Analysis

The fatigue life of any fabricated steel structure can be described using the following three factors:

- the range of stress at the detail under examination;
- the number of cycles of loading at the detail;
- the detail classification.

Although some comments will be made in this paper about the first two issues, attention will be focused on the detail classification, especially as it applies to riveted shear splices.

All fabricated steel structures contain metallurgical or fabrication-related discontinuities, and most also include stress concentrators such as weld toes. Consequently, fatigue failure is usually the result of slow crack growth from an existing discontinuity at a stress concentration. A description of the fatigue crack growth phenomenon can be made on the basis of a fracture mechanics model [1]. However, it is not practicable to use the fracture mechanics approach in design, and almost all design specifications simply arrange standard structural details into categories relative to their expected fatigue life. The expected fatigue life is established on the basis of test results, sometimes aided by fracture mechanics examination and sometimes requiring engineering judgement.

2.2 Fatigue Failure in a Riveted Connection

For a riveted connection, the experimental evidence is that in shear splices the great majority of fatigue failures relate to the connected material, not the rivet itself. Thus, the fatigue life can be expected to be a reflection of such features as the size of the hole relative to the part, the method of hole forming (drilled, punched, or sub-punched and reamed), the bearing condition of the rivet with respect to the hole, and the clamping force provided by the rivet group.

At the present time, the influences of clamping force, bearing condition, and the method of hole formation have not yet been examined in any systematic way. The influence of the hole size, *per se*, is not likely to be a strong one as long as the hole sizes and plate thicknesses normally used in structural practice pertain. Thus, the best data available are tests on riveted connections of proportions that are consistent with usual structural practice and are of full size, or at least large size. For the time being, the effects of clamping force, bearing condition, and hole formation must simply be part of the data pool. For this reason, and because the "defect" presented by a riveted connection is not severe, it is to be expected that the scatter of data will be relatively large.

2.3 Treatment of Riveted Details in Representative Standards

Not all specifications address the fatigue life evaluation of riveted connections. The short review that follows is not intended to be comprehensive, although it is believed to be representative.

Eurocode 3 [2]— Riveted shear splices are not mentioned in this standard. If it is assumed that a riveted shear splice is the same as a splice that uses non-preloaded high-strength bolts, then Eurocode 3 prescribes the use of Detail Category 112. The slope of the fatigue life vs. number of cycles is taken as 3 until the constant amplitude fatigue limit is reached (which is at 5 million cycles). For Detail Category 112, this corresponds to a stress range of 83 MPa. A slope of 5 can then be used until the cutoff limit is reached (100 million cycles, 45 MPa). The Eurocode rule is plotted in Fig. 1, together with the test data that will be described later.

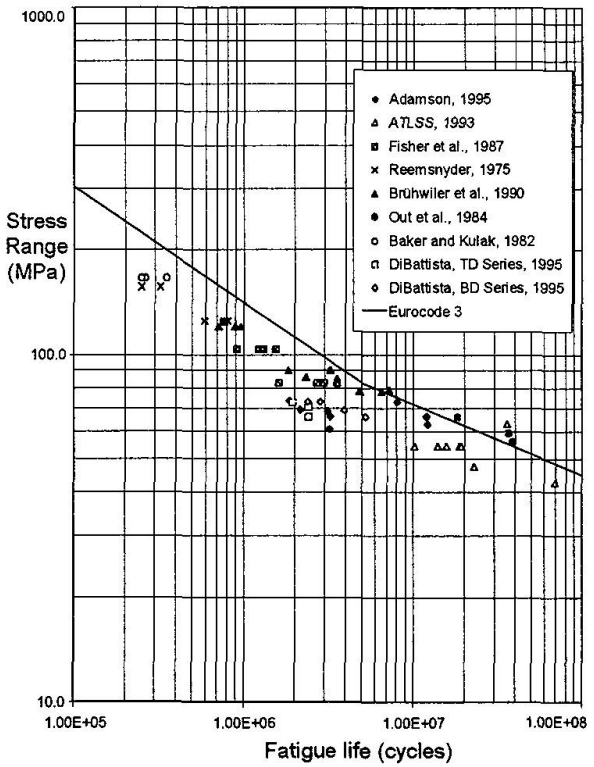

Fig. 1 Test Results + Eurocode 3

British Standard (BS5400, Part 10) [3] — With the advent of the EUROCODES, development of national standards in Europe has ceased. However, riveted shear splices are specifically mentioned in BS5400, and it is likely that the information is still being used. The riveted shear splice detail is described in BS5400 as their Class D. A slope of 3 is used until the constant amplitude stress range of 53 MPa is reached at 10 million cycles. If variable amplitude cycles are present in this low stress range region (likely the case with a bridge), then a slope of 5 is used for all stress ranges less than 53 MPa. Figure 2 shows the permissible fatigue life rule and the test data.

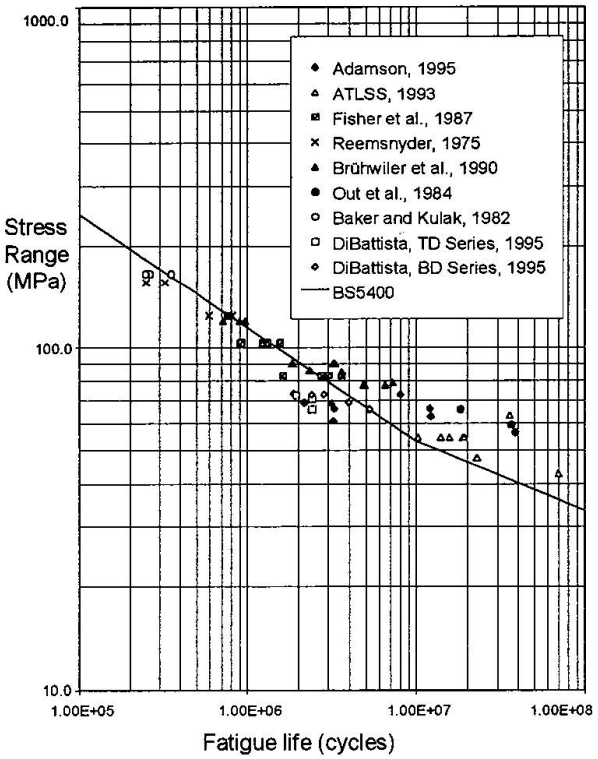

Fig. 2 Test Results + BS5400

American Association of State Highway and Transportation Officials (AASHTO) [4] — Riveted shear splices are designated as AASHTO Category D. The stress range vs. number of cycles relationship has a slope of 3 and the constant amplitude stress range is 48 MPa. If the effective stress range is below the variable amplitude fatigue limit (17.7 MPa), then it is assumed that no fatigue damage occurs for these stress ranges. Figure 3 shows the AASHTO permissible fatigue life rule and the test data.

American Railway Engineering Association (AREA) [5] — This standard is widely used by railroads in North America. Of the standards reviewed, it is the one that most closely reflects the recent test data, which are reviewed later in this paper.

The rules in the AREA Manual distinguish between cases in which it can be identified that the rivets are tight and have developed a normal level of clamping force and those situations in which the slip resistance is deemed to be low. No advice is given as to how the tightness is to be determined, however. If the decision is made that the slip resistance is low, then AREA Category D is to be used. At 2 million cycles, the permissible stress range for this category is 71 MPa. The slope of the fatigue life line is to be taken as 3 until the stress level of 41 MPa is reached, which occurs at 10 million cycles. Figure 4 shows the Category D line and the test data.

It would be more common to evaluate the fatigue life on the assumption that the level of clamping force in the rivets can be taken as "normal." In this option, the AREA rules provide two categories. When the holes might have been punched, the fatigue life is that of Category D (71 MPa permissible stress range at 2 million cycles) for any stress range above 62 MPa. For stress ranges just below 62 MPa, the fatigue life line is then shifted laterally until it hits the Category C line, after which it moves downward on that line until the variable amplitude fatigue limit of 41 MPa is reached. This is shown in Fig. 5. If the holes have either been drilled or were sub-punched and then reamed, a further improvement is available. This occurs in the region 53 MPa down to 41 MPa. See Fig. 6.

The AREA rules simply capture the boundary of the test data, as can be seen in these figures. The lengths to which this standard has gone to provide rules that are as close to the test data as possible reflects the importance of this region to owners: a large portion of the stress ranges experienced in North American rail operations are in the region of 40 to 70 MPa. For proper

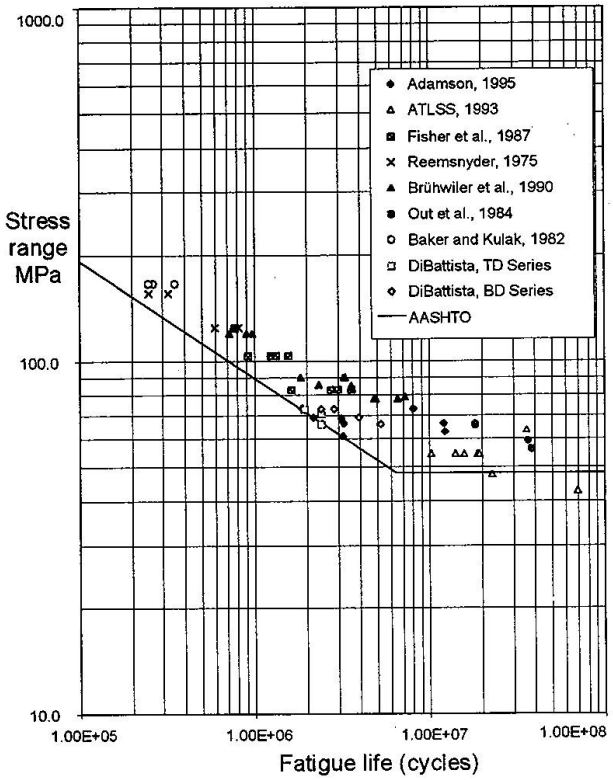

Fig. 3 Test Results + AASHTO

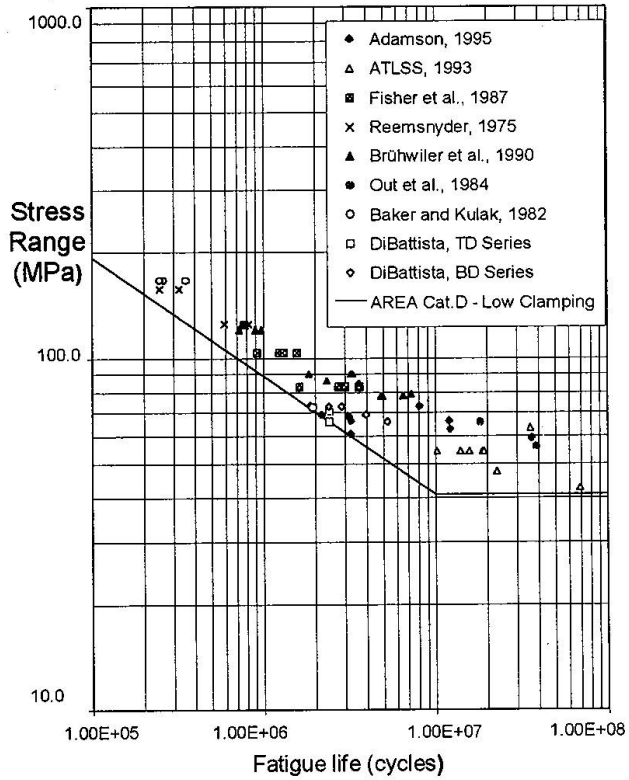

Fig. 4 Test Results + AREA, Low Clamping

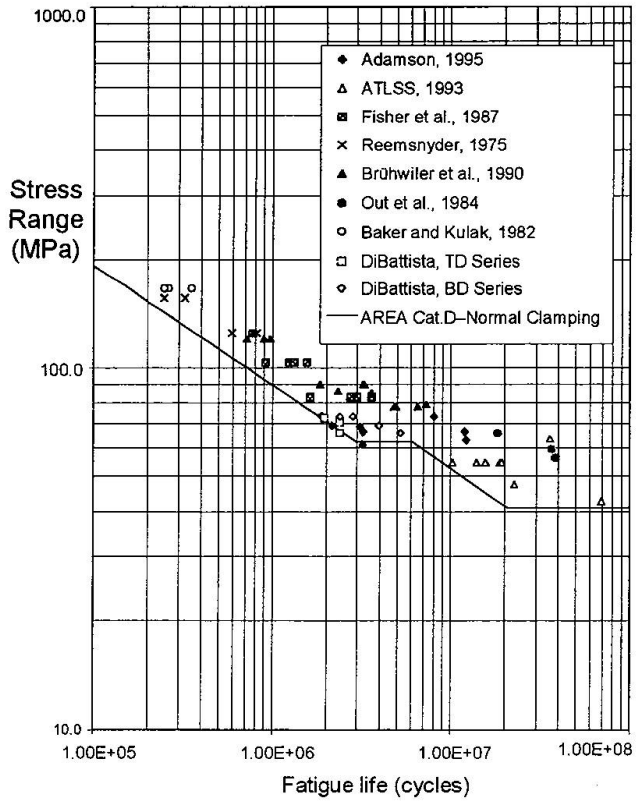

Fig. 5 Test Results + AREA, Normal Clamping

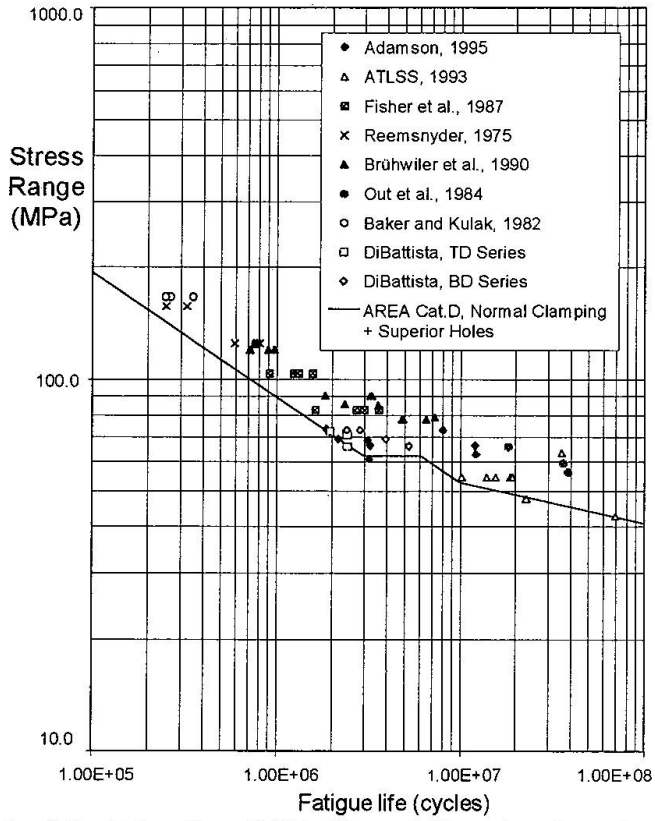

Fig. 6 Test Results + AREA, Normal Clamping, Superior Holes

evaluation of remaining fatigue life of existing bridges, it is of great importance to maximize the detail category in this region, while at the same time maintaining a suitable margin of safety.

In reviewing any of the design guidelines given in the foregoing summary, it is important to remember that the other components of a fatigue life evaluation—calculation of stress cycles, loading history, stress counting methods, and so on—are not necessarily the same in the standards cited.

3. Fatigue Test Data for Riveted Shear Splices

3.1 Fatigue Life Data

The fatigue life data shown in Figs. 1 to 6 (the data are identical in each figure) come from a variety of sources. In most cases, the members tested were taken from a structure that had been in service. Most specimens were tested in constant amplitude fatigue. All specimens were full-size. Details of the actual test conditions and member configuration must be obtained from the original source material. A brief description of the tests follows.

- Reemsnyder 1975 [6]: Full-scale fatigue tests on truss chords that had riveted gusset plate connections. The critical detail was that of the connection between the tension chord and a gusset plate.
- Baker and Kulak 1982 [7]: Full-scale fatigue tests on built-up hanger members. The arrangement was such that the rivets were not subject to any shear force, and thus the bearing stresses in the connected material were negligible.
- Out *et al.* 1984 [8]: Flexural tests on built-up railway stringers (beams) in which flange angles were riveted to a web plate. The critical detail was the continuous riveted connection between the web and the flange angles, and it was located in a region of constant moment.
- Fisher *et al.* 1987 [9]: Flexural tests on built-up railway stringers (beams) in which flange angles were riveted to a web plate. The configuration was similar to that of Out *et al.* except that a coverplate riveted to the outstanding leg of the flange angles was also present.
- Brühwiler *et al.* 1990 [10]: Tested riveted built-up plate girders, riveted lattice girders, and rolled mild steel girders that had a cover plate riveted to the flanges.
- ATLSS 1993 [11]: Flexural tests on built-up railway stringers (beams) in which the flange angles were riveted to the web plate. The critical detail was the continuous riveted flange-to-web connection.
- Adamson and Kulak 1995 [12]: Flexural tests on built-up railway stringers (beams). The configuration was similar to that described in the ATLSS 1993 program.
- DiBattista and Kulak 1995 [13]: Tension tests on diagonals taken from a railway truss bridge. The designations TD and BD refer to the connection at the top or the bottom of the member and reflect the way the net area is calculated. See the original source material. The cross-section of the member consisted of four angles connected to a web plate. The critical detail was the connection of the outstanding legs of these angles to gusset plates.

3.2 Evaluation of Fatigue Life Rules

Figures 1 through 6 contain the test data deemed to be most relevant for evaluation of the fatigue life of riveted shear splices and the individual fatigue life rules. The following observations can be made.

Eurocode 3 —Use of a standard that does not specifically mention riveted shear splices can be criticized as inappropriate. However, there are a number of standards in force that do not mention riveted connections, and it may be that a decision has to be made by the designer as to a suitable category. In this case, Detail Category 112 appears to be a reasonable choice based on the information in the standard. Since the failure mode anticipated is cracking in the net section of the connected material, the strength of the fastener (i.e., rivet versus bolt) is not relevant. Non-preloaded high-strength bolts, which are specifically permitted by this standard, are in principle no different than a rivet with respect to fatigue of the connected material. Thus, it appears that selection of this detail category for use with a riveted shear splice is reasonable within Eurocode 3.

From the information in Fig. 1, it is obvious that use of Eurocode Detail Category 112 is not suitable for use as a predictor of the fatigue strength of riveted shear splices. The prediction line greatly overestimates the fatigue life.

British Standard (BS5400, Part 10) — Unlike the Eurocode 3 standard, this standard does distinguish between riveted shear splices and bolted shear splices. However, Fig. 2 shows that the fatigue life rule provided by this standard for riveted shear splices also is not satisfactory.

AASHTO — This standard also provides fatigue life rules for each of bolted and riveted shear splices. As seen in Fig. 3, the predictor line is a reasonable boundary to the test data, except for two data points at long lives (approximately 20 and 70 million cycles). It was noted earlier that the variable amplitude fatigue limit is given as 17.7 MPa. If that limit were to be used, the rule would capture these data, but it would be too conservative. Alternatively, it has been suggested (unpublished correspondence) that the AASHTO Category D line should be extended downward to a fatigue limit line at 41 MPa. This would be a reasonable choice, and it is the solution presented in the AREA rules, described following, for the case where slip resistance is deemed to be low. (Figure 4, which relates to the AREA rules, shows how such a fatigue life line would look relative to the test data.)

AREA — It has been described earlier that the AREA rules offer three choices for fatigue life of riveted shear splices. If the clamping force provided by the rivets is considered to be low, then their Category D is used, along with a fatigue limit line at 41 MPa (Fig. 4). All of the test points lie on or above this line. It is therefore a satisfactory solution, except that it might be that it is too conservative in the region of the knee of these two lines. More tests in this region would be helpful. Another solution, which will be discussed later, is to provide a transition fatigue life line between the two parts of the bi-linear fatigue life prediction shown in Fig. 4.

The second choice offered by the AREA specification is depicted in Fig. 5. This case is described as applicable to conditions of "normal" clamping, and it is also intended to be used when it can only be assumed that the holes were punched. The fatigue life line shown in the figure has been selected to generally skirt the test data. It can be criticized on the basis that the prediction might be too generous in the region between, say, 4 million and 20 cycles. (Small changes in the placement of the predicted curve in this region can have a large impact on the fatigue life predicted.) As observed earlier, more test data in this region (at stress ranges less than about 60 MPa) are desirable. The possibility of using a transition curve can also be considered here.

The other choice available in the AREA specification is shown in Fig. 6. It is intended for use when it is known that the holes were either drilled or sub-punched and reamed. This prediction follows the lower boundary data points even more closely than the one shown in Fig. 5.

4. Issues Arising from the Examination of Rules and Data

4.1 Failure Criterion

A review of various experimental data reveals that not all researchers used the same criterion to define when fatigue failure of the member had taken place. Some reported the number of cycles to failure at a certain deflection criterion, some used the time at which the loading system was no longer stable, and some used cracking of an element as the basis for reporting fatigue life. In the last case, cracking could be the first detection of a crack or some later stage of cracking.

If the number of cycles is large, there might not be much difference between the various criteria. However, for shorter lives the distinction could be important, and of course it is generally desirable that all similar research results be reported on the same basis. The author suggests that cracking be used as the basis of reporting fatigue life. Based on the tests done by the author and his colleagues [12, 13], it is suggested that the fatigue life be reported as the number of cycles at the time the first crack has severed the element in which it appeared and a new crack has just started in a second element. For a tension member, the work of DiBattista and Kulak [13] showed that there will be relatively few cycles between this point and complete destruction of the member.

In riveted flexural members there will be more time between the point at which the failure criterion is reached and complete destruction because the cross-section is not uniformly stressed, as it is in the case of a tension member. As the crack grows, say from a bottom flange angle, the stress range will tend to decrease because the crack is moving upward in the member, but it will tend to increase because the amount of cross-section available to carry the forces is reduced. Overall, the failure criterion suggested seems to work well in these cases [12].

The proposed failure criterion was used in plotting the data in Figs. 1 to 6 whenever possible. This included at least the results from ATLSS [11], Adamson and Kulak [12], and DiBattista and Kulak [13].

4.2 Tension Members vs. Bending Members

The discussion about failure criteria has pointed out that the presence of a fatigue crack in a tension member is likely to be more serious than one in a flexural member. At the present time there are not enough data in each category to be able to separate the two groups, however. For the time being, all the data must be used together, but the consequences of fatigue cracking in each of these two different types of members should be kept in mind.

4.3 Effect of Staggered Hole Patterns

The limited amount of experience available shows that fatigue cracking will take place more or less orthogonally to the direction of the stress, even in the presence of a staggered hole pattern. This suggests that a cross-sectional area normal to the direction of the tensile stress in the member be used for the calculation of the stress range. However, it is reasonable to expect that the effect of staggered holes will be to increase the stress range that is driving the crack. One alternative then is to account for the effect of staggered holes as is done for static loading. Another option is simply to deduct both the holes in the plane of the crack and the full effect of the "staggered" holes, assuming that they are reasonably close to those in the plane of the crack. This was the option selected in calculating the stress range for the TD Series of DiBattista. (This means that the TD Series of DiBattista plot higher than they would using either of the other two alternatives. In Fig. 3, for example, the three TD points would plot below the fatigue life line of AASHTO if either of the other criterion were used.) The problem of just how to calculate the stress range in the presence of staggered hole patterns requires further investigation.

4.4 Criterion for Selection of a Fatigue Life Limit

It has been customary in selecting a fatigue life limit to use the mean less two standard deviations of the data (on the number of cycles). If the number of data is reasonably large, this means that the confidence limit is approximately 95%. The scatter in the riveted splice data is much greater than usually seen with welded details, however. So far, it has been usual to select a fatigue life line that is more or less at the lower limit of the data, such as has been done in the AREA standard [5]. There seems to be no reason to change this approach at the present time.

4.5 Improvement of the Fatigue Life Limit Selection Process

The bi-linear fatigue life representation used in most standards is a reflection of the simplification usually applied to the crack growth model, which is assumed to be bilinear. Kunz [14] has proposed that a transition be recognized between the crack growth region described by the Paris law and the threshold stress intensity value. Application of this produces a similar transition between the sloping and horizontal portions of traditional fatigue life curves. This provides a better representation of test data in the region of the "knee" of the traditional fatigue life curves. This idea could be easily incorporated in a design standard and it should be explored further.

Kunz [14] has also proposed that the limit below which no crack propagation occurs is not a constant, but decreases with increasing damage (crack growth). This fracture mechanics approach to forecasting fatigue life offers the possibility of improved predictions, particularly when variable amplitude stress cycles are present. This, too, should be explored further.

5. Summary and Conclusions

The selection of a fatigue life category for riveted shear splices can now be made on the basis of a reasonable amount of data derived from full-size tests. The review of a representative number of existing design rules has shown that improvement is needed in some cases. The author makes the following recommendations:

- A suitable fatigue life category for riveted shear splices is that shown in Fig. 4.
- An improvement to this selection in the important region of the knee of the bi-linear representation can be made using the work of Kunz [14].
- The fatigue life of riveted shear splices should be reported as the number of cycles at the time the first crack has severed the element in which it appeared and a new crack has just started in a second element.

The author also makes the following suggestions for research that will improve the understanding of fatigue life predictions for riveted shear splices:

- The influence of bearing stress upon fatigue life.
- The influence of rivet clamping force.
- The effect of staggered hole patterns on fatigue crack growth.
- The influence of method of hole forming upon fatigue life.

References:

1. Broek, D. (1989). *The Practical Use of Fracture Mechanics*. Kluwer Academic Publishers, London.
2. European Committee for Standardisation (1992). *Eurocode 3: Design of Steel Structures*, ENV 1993–1–1, Brussels.

3. British Standard BS 5400, Steel, Concrete and Composite Bridges (1980). *Part 10, Code of Practice for Fatigue.* British Standards Institution, London.

4. American Association of State Highway and Transportation Officials (AASHTO) (1992). *AASHTO LRFD Bridge Design Specifications*, SI Units, First Edition, Washington, D.C., 1994.

5. American Railway Engineering Association (AREA) (1996). *Steel Structures.* Chapter 15, Manual for Railway Engineering.

6. Reemsnyder, H.S. (1975). *Fatigue Life Extension of Riveted Connections.* Journal of the Structural Division, ASCE, Vol. 101, No ST12, pp. 2591-2608.

7. Baker, K. A. and Kulak, G. L. (1982). *Fatigue Strength of Two Steel Details.* Structural Engineering Report No. 105, Department of Civil Engineering, University of Alberta, Edmonton, Canada.

8. Out, J.M.M., Fisher, J.W., and Yen, B.T. (1984). *Fatigue Strength of Weathered and Deteriorated Riveted Members.* Transportation Research Record 950, Transportation Research Board, National Research Council, Washington, D.C., pp. 10-20.

9. Fisher, J. W., Yen, B.T., Wang, D., and Mann, J.E. (1987). *Fatigue and Fracture Evaluation for Rating Riveted Bridges.* National Cooperative Highway Research Program Report 302, Transportation Research Board, National Research Council, Washington, D.C.

10. Brühwiler, E., Smith, I.F.C., and Hirt, M.A. (1990). *Fatigue and Fracture of Riveted Bridge Members.* Journal of Structural Engineering, ASCE, Vol. 116, No. 1, pp. 198-214.

11. ATLSS (Center for Advanced Technology for Large Structural Systems) (1993). *Assessment of Remaining Capacity and Life of Riveted Bridge Members.* Draft Project Report to Canadian National Railways, Lehigh University, Bethlehem, Pennsylvania.

12. Adamson, D.E. and Kulak, G. L. (1995). *Fatigue Tests of Riveted Bridge Girders.* Structural Engineering Report No. 210, Department of Civil Engineering, University of Alberta, Edmonton, Canada.

13. DiBattista, J.D. and Kulak, G.L. (1995). *Fatigue of Riveted Tension Members.* Structural Engineering Report No. 211, Department of Civil Engineering, University of Alberta, Edmonton, Canada.

14. Kunz, P. (1992). *Probabilistic Method for the Evaluation of Fatigue Safety of Existing Steel Bridges.* Doctoral Thesis No. 1023, ICOM – Steel Structures, Swiss Federal Institute of Technology, Lausanne, Switzerland.

Acknowledgment

This paper is a shorter and slightly different version of material published under the same title in *Stahlbau 31*. The permission of the Editors of Stahlbau to adapt the material for use in this paper is acknowledged with thanks.

Full Scale Laboratory Fatigue Tests on Riveted Steel Bridges

Rosemarie HELMERICH
Civil Engineer
BAM
Berlin, Germany

R. Helmerich, born in 1954, received her degree in civil engineering from the Technical University Bratislava, Slovakia. After working in the fields of reconstruction of industrial buildings and materials testing, since 1990 she is working in the field of research of steel structures at BAM.

Klaus BRANDES
Dr.-Ing.
BAM
Berlin, Germany

Klaus Brandes, born in 1936, received his degree as well as his doctorate from the Technical University of Berlin. After working for some years in the field of steel structures, he went to the Federal Institute of Materials Research and Testing (BAM) in 1968 where he is concerned with various fields of structural engineering

Jürgen HERTER
Civil Engineer
BAM
Berlin, Germany

Summary

Thousands of old riveted structures, made of wrought iron as well as early mild steel are still in service. However, the fatigue behaviour of deteriorated riveted steel bridges is not well understood. In this paper we present the results of full scale tests on large members and parts of riveted bridges built between 1890 and 1906. The tests on three types of riveted bridge include strain measurement under traffic loads, full scale laboratory tests and small scale or Non Destructive Testing methods (NDT). Advanced material investigations have been carried out, including crack propagation tests, fracture toughness tests and tensile tests.

1. Introduction

It is well known that a great number of old bridges are still performing now as they did 100 years ago. There is often a need to keep them in service because of economic reasons or as historical monuments. Extending the life of a bridge requires knowledge of crack growth behaviour in order to assess the future safety of a given bridge against fatigue damage during its future life.

The paper presents only a first step, but the results obtained can be used to develop rational rating concepts through knowledge of critical structural details, crack growth behaviour of details with built-in defects and the influence of the low fracture toughness which is common to wrought iron elements and whole bridges. We introduce advanced assessment methods using NDT and small destructive techniques based on our experience during full scale laboratory tests and site testing on the same bridges under traffic loads before they were decommissioned.

For thousands of old steel bridges built between 1850 and 1900 riveting was the only connection method. Structural members were normally built up from many relatively thin plates (< 15 mm) or angle sections. Wrought iron has proven to be resistant to corrosion because of its layered structure. Consequently, such structures are more redundant and are not as susceptible to corrosion as more recent materials. Residual stresses as found in modern welded structures created by high temperature differences during the welding procedure are not found in riveted

structures. Nonetheless, riveted bridges may have been war damaged or subjected to impact by lorries or cranes, producing defects in the structure which are not easily visible.

During the 1890's in Germany calculation methods using allowable stresses for static loading up to 105 N/mm^2 and for traffic loads up to 70 N/mm^2 were adopted in design (Hütte, 1892). In the course of time, for example during wartime, old bridges were subjected to higher loading than they were designed for, because of increased axle loads and heavier war traffic. It is often very difficult to determine the load history of these old structures.

Most test results reported in the literature are based on small test specimens in order to get information about material behaviour under fatigue loading or the behaviour of a connection. At BAM, we performed three series of full scale tests in order to determine the fatigue critical details in a girder or a steel bridge and to investigate fatigue crack initiation at specific points. These tests allowed a study of the special effects of fatigue loading in a structure when the cross girders are not removed from the structure to be tested independently. Full scale tests in Lausanne and Karlsruhe reported in the literature have been taken into consideration in the assessment of our results. The results of our tests have been used in order to adapt methods for crack identification by NDT as the basis for using a fracture mechanics approach in the bridge rating procedure.

2. Full scale tests

2.1 *Configuration of the test specimen*

All bridge elements tested have been taken from three bridges in Berlin. The first bridge, built in 1902 on the Berlin Underground railway U 1, was made of early mild steel and had been in good condition with respect to corrosion. Figure 1 shows the testing arrangement for the first specimen, a main truss girder, which was supported such that the cyclic load was applied to the end of a cantilevering section of the girder, as shown in Fig. 1A. Two girders of this type have been tested.

The second specimen was a web plate girder taken from a road bridge crossing the Teltow canal between Berlin and the former GDR. Built in 1906 during the construction of the canal, the bridge was 40 years out of service, but obviously in relatively good condition. The bridge was made of mild steel. It has been taken out of service because the bridge was too small after unification of Germany in 1990. The two point loading test arrangement of the 10 m long cross girders is shown in Fig. 1B. Three girders of this type were tested.

Lastly, a suburban train bridge made of wrought iron built in 1890 has been tested. The bridge was cut into three parts transversely so that the cross girders remained connected to the main girders. Each part of the bridge was supported on the main girders, and a two point test load was applied to the cross girders in order to study their behaviour under the real loading and end-connection conditions (Fig. 1C). Four cross girders of this type were tested.

The full scale tests were followed by tension tests, chemical analysis, crack growth tests and microstructure analysis. Details are available in the BAM test reports.

2.2 Equipment and test method

All test specimens were subjected to constant amplitude load cycles. The nominal stress ratio was 0.1 in all tests. The maximum stress difference had to be higher than 71 N/mm^2, corresponding to the ECCS 71 detail category (AASHTO D). Our main goal was to get results for high stress ranges in the region of the transition from m=3 to m=5 on the S- N (Wöhler) curves.

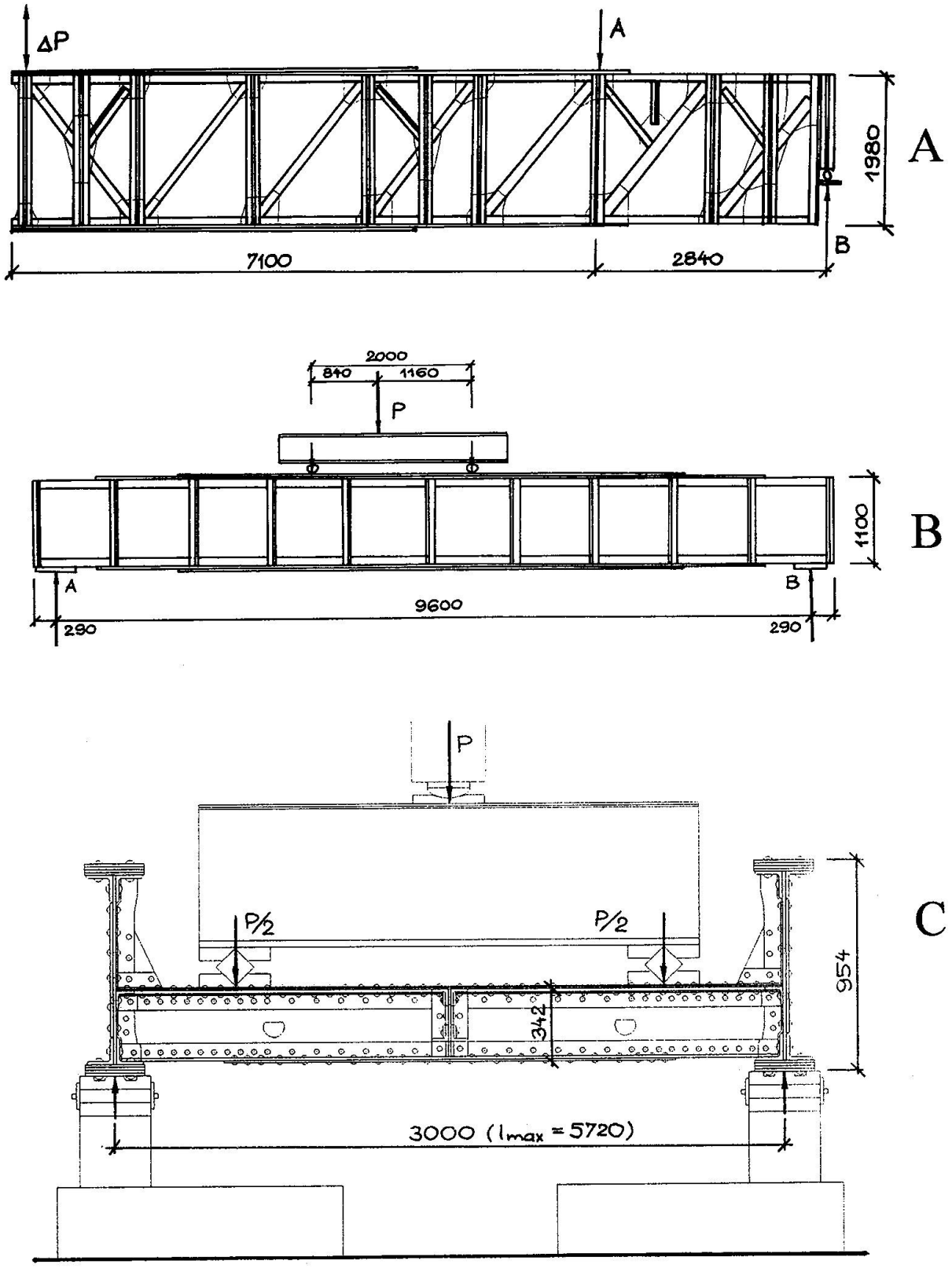

Fig. 1 *Load arrangements :* **(A)** *main truss girder,* **(B)** *riveted plate cross girder, and* **(C)** *bridge parts made of wrought iron*

We did not take into account the load history of the bridges during the tests because the measured strain range under traffic loading was low. During the first and the third test series we had the opportunity to measure strains under suburban train traffic before the bridges were dismantled. Measured maximum stresses under traffic loading were lower than 29 N/mm^2 for both bridges. According to fracture mechanics, these stresses cannot initiate or propagate cracks, although later they are taken into consideration for discussing the test results. The third bridge was in service for less than 40 years.

Individual tests were terminated either at an increase of the maximum deflection of more than 0.2 mm between measurements or once a crack propagated through the entire section of a element. In some of the tests, the test was continued until the crack grew into the web plate.

The girders from the second series were cut into smaller specimens (lengths of about 1m) and the fatigue tests were continued with the same load range as in the main tests. These results are included in Fig. 8. During the third test series (wrought iron), we continued the test on a cracked element at the stress level which was measured under traffic load.

3. Results

3.1 Material investigations

The materials were analysed by several tests. **Tensile test**: Except for the truss girder (gusset plate) all standard test specimens were provided only in the main rolling direction. All results are summarised in Table 1. The yield stresses of mild steel and wrought iron do not differ very much. The Young's modulus of wrought iron is on average about 10-15% lower than that of mild steel; in the tests we got a value of about 195 000 N/mm^2, which is similar to results from literature and old scientific papers written in the for last century. This Young's modulus has been taken for calculating stresses in our wrought iron tests. Ultimate elongation is lower, and in particular, macroscopic necking does not occur. This behaviour is a consequence of the microstructure of wrought iron. Wrought iron behaves like a composite material with layers of ductile ferrite matrix with brittle slag layers. This structure is a result of the forging and rolling process.

The **microstructure** at the crack- tip- opening region for mild steel and wrought iron was investigated. Fatigue striations for the length of a crack during one load cycle were found on the fracture face in both materials. In mild steel, for example, a crack was stopped and divided into two tip- cracks in the CTO- region after leaving the rivet head because of the material's ductile behaviour. In wrought iron a split level (terrace) crack was found in a web plate after finishing the test; the crack was not visible from outside. This crack showed typical nodal lines stepped in the plates area.

Crack growth tests of wrought iron were carried out. In these tests, the influence of lower temperatures was not taken into consideration. All test results for cracks perpendicular to the rolling direction were below the Barsom curve for contemporary steels. Rolfe and Barsom (1987) proposed this empirical approximation for steels with a yield strength greater than 250 N/mm^2. Test results are shown in Figure 2 in relation to this curve. Tests for cracks oriented parallel to the rolling direction produced results above this curve, meaning that such cracks propagate faster. The cyclic stress intensity ΔK depends on the stress range; a higher stress range results in a lower cyclic stress intensity. The yield cyclic stress intensity ΔK_{th} of the investigated wrought iron was ~ 10 MPa·m$^{1/2}$ for a nominal stress ratio of 0.1.

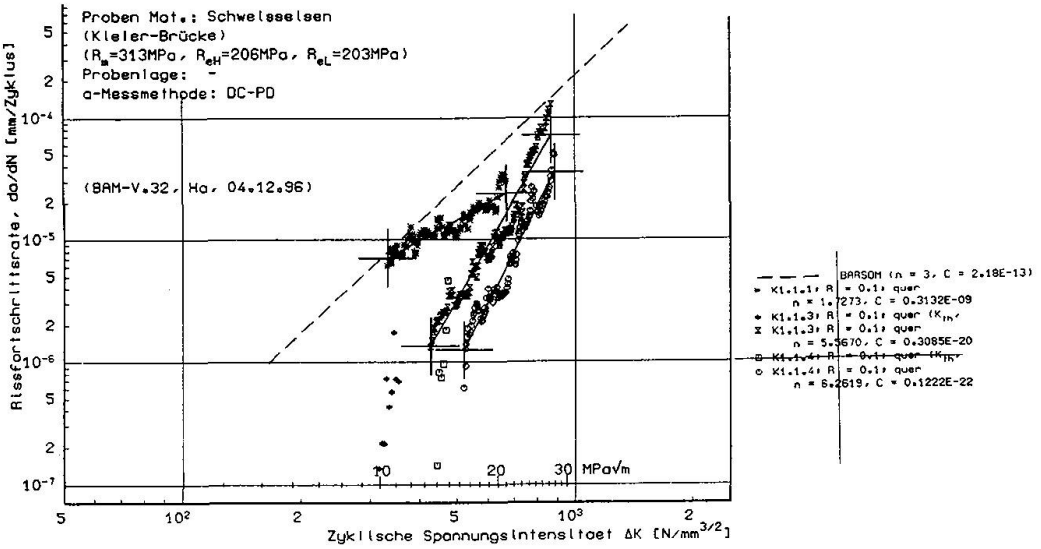

Fig. 2 Results of crack growth tests on wrought iron specimens

Material	Higher Yield Stress N/mm²	Lower Yield Stress, σ_Y N/mm²	Ultimate Tensile strength, σ_f N/mm²	Ultimate Elongation %	σ_Y/σ_f
1. Test, WB mild steel, 1902,	underground - 16 specimens	suburban line U1			
Mean in rolling direction	255	234	446	29,5	0,57
standard deviation s_x	25,4	23,3	10,8	2,4	
Mean 90° to rolling direction	244	236	442	27,5	0,55
standard deviation	19,5	17,3	7,9	1,6	
2. Test, Kn mild steel, 1906	road bridge				
Mean, angle profile (n=6)	321	296	371	17	0,86
standard deviation	11,1	3,0	6,4	3,1	
Mean, cover plate (n=12)	234	214	322	23,3	0,73
standard deviation	16,7	9,3	6,1	6,0	
3. Test, wrought iron, 1890	suburban line 5 specimens				
Mean, angle iron	243	233	339	15,5	0,72
standard deviation	2,82	14,58	24,0	2,6	
Mean, cover plates	211	207	315,6	18	0.67
standard deviation	7,3	5,6	7,4	2,7	

***Table 1** Tensile test results*

3.2 Results of fatigue tests

The results of all fatigue tests are given in Table 2. Only one truss girder (Suburban train viaduct, U1,mild steel, WB1, main girder) was repaired and the test was continued with the same maximum strain difference. The fatigue failure occurred in an untypical net cross-section on a hole drilled for a conveyer mechanism during dismantling. In the second test series (Road bridge, mild steel, Kn1-3, cross girder) a fatigue crack occurred in the constant moment region. For the wrought iron bridge test series (Suburban train bridge, S1, Kie 1-4), the cross girders were tested under their original support conditions. (Bridge parts up to 3,3m x 5,70m were supported at four points on their main girders).
All results fall in a S-N diagram above the ECCS category 71 with constant slope m = 5.

Te st specimen	Net cross-section range, Ds	Numbers of cycles Mio cycles	Crack location (first cracked element)
	N/mm^2		
(A) truss girder,	**mild steel, 1902**		
WB 1	80	2,600	at a new drilled hole (untypically, repaired)
WB 1,continued	80	3,600	in a gusset plate
WB 2	140	0,250	in a gusset plate
(B) plate girder	**mild steel, 1906**		
Kn 1	101	2,618	second cover plate, at rivet hole (in built failure)
Kn 2	123	0,361	second cover plate, at rivet hole (outside impact damage)
Kn 3	115	0,562	second cover plate, at rivet hole
(C) plate girder bridge	**wrought iron, 1890**		
Kie 1	130	0,586	at rivet hole under cutoff in web- plate
Kie 2	108	2,829	at rivet hole, angle on the end of a cower plate
Kie 3	97	2,691	at rivet hole, angle on the end of a cover plate
Kie 4	104	4,008 4,276	+ 0,2mm- at rivet hole under a cutoff in web- plate, (rivets on plates ends of the cross girders were replaced by prestressed bolts)

Table 2 *Results of full scale fatigue tests*

3.3 Characteristics of crack initiation and geometry of growing cracks

In all tests we noticed that crack initiation was not detectable. All cracks were identified by increasing strains or deflections, or after they reached the edge of an element. Most of the cracks were initiated at rivet holes, often caused by changes in the cross-section geometry. Stress concentrations may also occur at hidden defects within a built-up section. In the tests we also discovered cracks at such defects.

In the **truss girder** test series all fatigue cracks occurred in the gusset plates, indicated by increasing strains during the test. The cracks initiated in the region of the gusset plate near to the last rivets on the diagonal where the gusset is sandwiched between two diagonal elements. Details of the gusset plate with the crack after removing rivets and the diagonal elements are shown in Figure 3. After elongation of the rivet hole cracking began at the edge of the rivet hole. Additional factors contributing to crack growth, for example from rivet installation, were not found in our tests. As known from literature, at this time (1902) in Germany rivet holes had to be drilled; punching was not allowed in structures with traffic loads. Exceptions to this rule might have occurred.

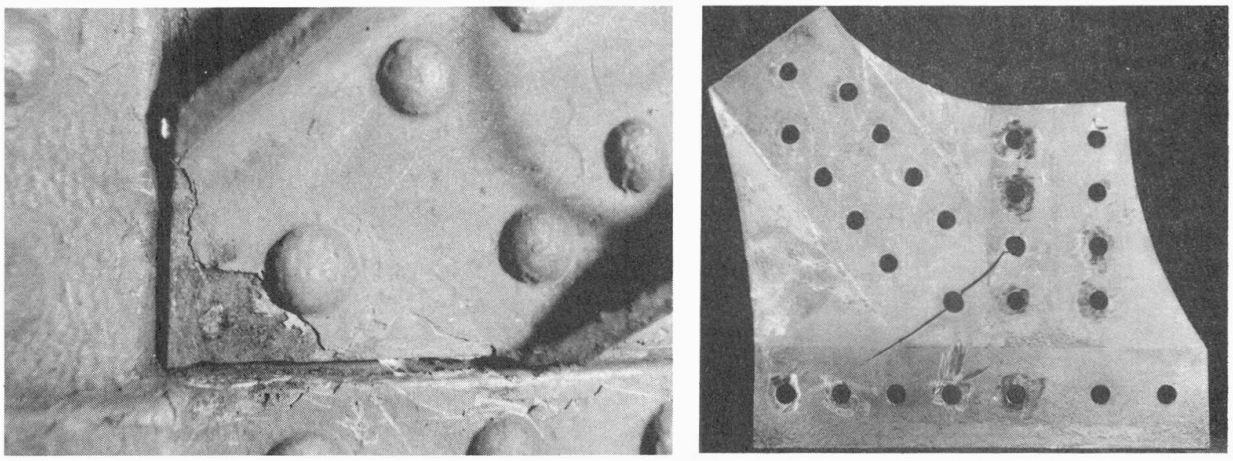

Fig. 3 *Details of a cracked cover plate* ***(A)*** *concealed within the structure,* ***(B)*** *after disassembly*

In the **plate girder** test series (mild steel, 1906, Kn), all cracks initiated in the cover plate, sandwiched between angles and additional cover plates. Cracks were found after deflection and strains increased or when the crack was long enough to reach the edge of the sheet plate. When cracks reached the edge, they were only visible when the girder was loaded. All tests were continued to find out if crack growth became unstable. The result was plastification at the crack tip and crack dividing into two tips, but no unstable growth. In one of these tests the crack tip in the web plate had been cooled down to -30°C on both sides of the web plate. The crack tip detail is shown in Figure 4.

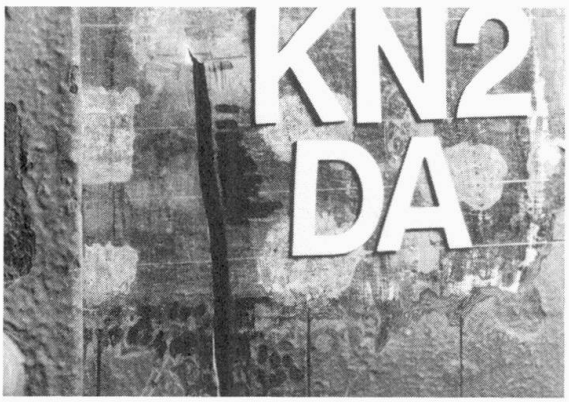

Fig. 4 *Detail of crack tip in a web plate*

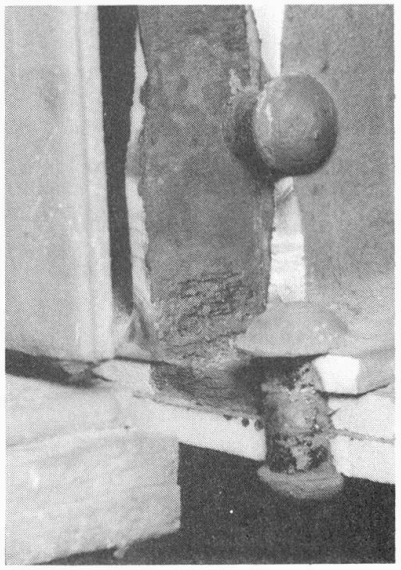

Fig. 5 *Crack in the tension flange*

The bridge crossing the Teltow canal "Knesebeck-bridge ", had presumably been damaged during World War II. Almost every bridge crossing the canal had been blasted during the last days of the war. We found old corroded failures in the cross section of cover plates and untypical cracking behaviour in the region of constant moments. In the tension flange of the second plate girder the crack was growing from an old corroded failure, as shown in Figure 5. The third web plate girder seemed to have been exchanged. In material tests we found higher tensile strength, appropriate to Fe 360, in girder Kn 3. By means of strain measurement or deflection measurement it was possible to detect crack growth.

In the third test series on parts of a **wrought iron plate girder bridge** (1890), typical for the Berlin Suburban railway, cross girders under their original support conditions were tested. Due to its special layered microstructure, unlike modern steels, the behaviour of wrought iron under constant amplitude fatigue load needs more tests. During the tests, in addition to strain and deflection measurements, we used Non Destructive Test methods such as magnetic particle tests, fibre optic sensors glued to the tension flange, an Acoustic Emission System and X-ray methods to detect cracks as early as possible. Initial readings from strain gauges taken every 15 minutes (1800 load cycles) indicated increasing strains. The optical fibre sensor cracked when the crack reached the edge of the angle. At that time the crack was not visible under good lighting conditions without loading (Figure 6). In the test Kie 1 the angle cracked in an unexpected cross-section under a drilled hole for a rainwater pipe. On other similar bridges, holes of this type had been framed with angles. This was not the case with this particular hole. The crack was also detected by a change in direction of the main stresses on the cracked girder in the joint between main and cross girder, measured by means of strain gauge rosettes. A terrace crack in the web plate was found after finishing the test and disassembly of the girder (Figure 7). Crack tips in the angle were found only by magnetic particle tests or by X-ray. The crack was indicated by increasing strains, fretting rust and a cracked old paint layer near the crack. After the point at which the measured strain had increased by 1%, it took 47 000 further load cycles until the web-to-flange angle was craked. Relating to traffic load (max. 30 N/mm^2 in net cross section) it means on this bridge 4,3 years of service for one full train every 10 minutes until the tension flange is damaged, if it is not assumed that low load cycles do not cause crack growth. Magnetic particle testing also discovered misaligned rivet holes which had been back-filled in near to the cracked cross-section. However, no cracks were found at these back-filled holes.

In the last cross girder test, the last rivets of the cover plates were replaced by prestressed bolts. In this case, from the point at which strains had increased by 1%, it took 2 million high-stress-range load cycles until failure of the web-to-flange angle.

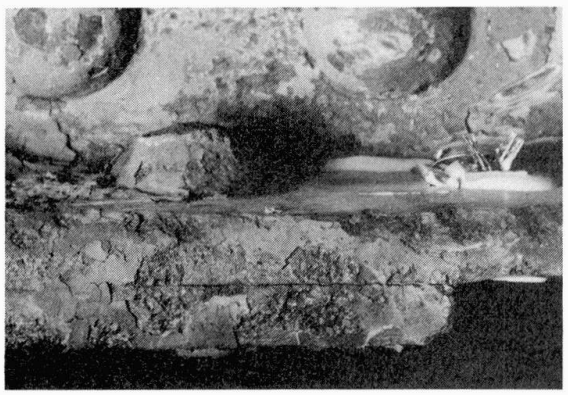

Fig. 6 *Cracked angle in tension flange*

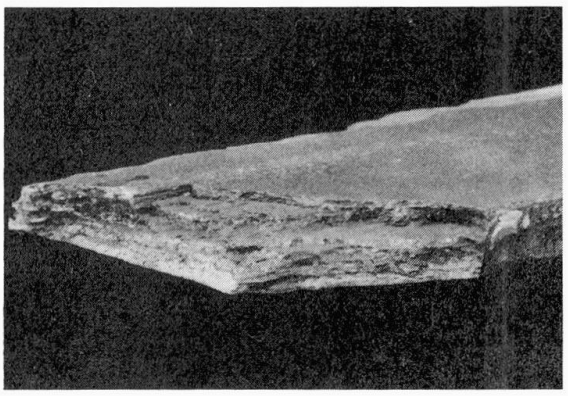

Fig. 7 *Terrace crack in web plate*

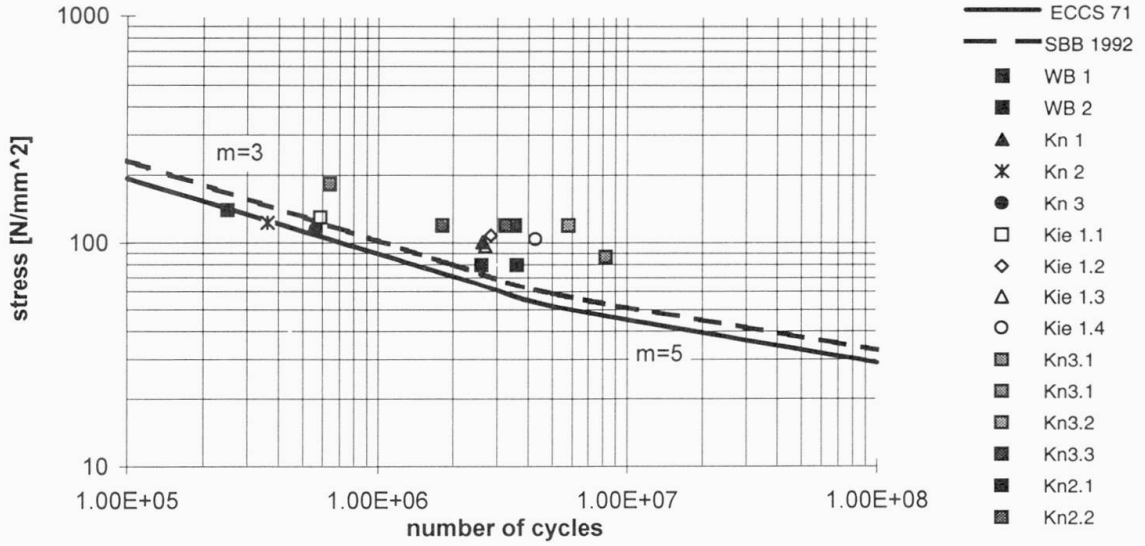

Fig. 8 *Results of full scale tests in S-N-curve*

In two tests the crack occurred in the plate under an additional plate at the first row of rivets. Crack growth was indicated by decreasing strains in the tension flange. All tests are summarized in the S-N-diagram in Figure 8.

4. Non Destructive Testing methods

Fig. 9 *Crack in a tension flange test Kie 3*

Non Destructive Testing methods such as **X-Ray** make it possible to see a crack on a film. However, more tests are needed to develop this method for applying it to bridges in service. First tests on the Berlin Suburban railway are finished. Figure 9 shows a crack in the tension flange of cross girder Kie 1.3 (scanned X-ray- film). Of course, these tests are possible only for special cross-sections under special conditions (40 m diameter safety zone) because of the X-Ray emissions.

Testing should be carried by NDT specialists under the direction of the investigating engineer. In most cases, the costs of testing are outweighed by the savings in structural repair or replacement costs.

For detection and location of damage in large parts of wrought iron bridges we used glued **fibre optic sensors**. An only primarily coated optical fibre was fastened to the top and the bottom side of the bottom flange of the cross girder. Because fatigue cracks were expected near rivet heads the fibres were sensitised (coating) in this area before gluing. A threshold limit for crack formation in the range between 10 and 200 μm can be obtained. This method is also a cheap way of detecting existing cracks with a width of between 10 and 30 μm which open under traffic loads and which cannot be detected visually. The measurements made with a fibre optic sensor during test Kie 1 detected a crack (after 628 000 load cycles) as shown in Figure 10.

Fatigue cracks were also detected using the **magnetic particle method**. This method was used during laboratory tests after strains changed in a certain region, and it has been used on bridges in service to find cracks and their direction in the region of war damage or highly stressed rivet heads.

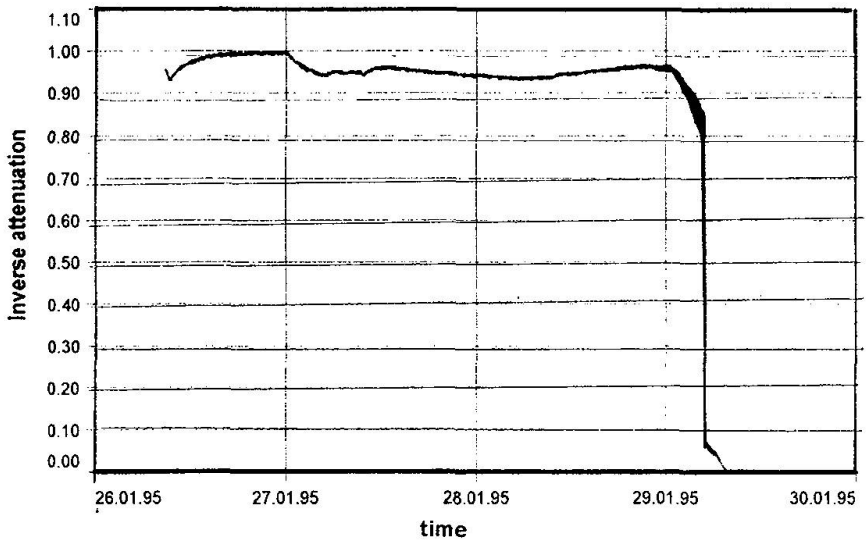

Fig. 10 Signal from a sensitised optical fibre before and after crack formation (Kie 1)

5. Concluding remarks

1. Results of testing riveted connections agree with the design code ECCS detail category 71 with slope m=5. Tests indicate that this detail category can be used for evaluating old bridges.

2. Some fatigue cracks initiated at old corroded impact damage or structural defects. Nonetheless, constant-amplitude fatigue limit detail category 71 N/mm^2 covers these test results.

3. Fatigue cracks which do not reach the edge of an element are not detectable unless NDT methods are used. The magnetic particle and X-ray methods enable the detection of existing cracks.

4. Cracks growing in tension elements can be indicated by a change in the direction of main stress, measured using strain gauge rosettes, for example during permanent tests on bridges.

5. The fatigue behaviour of wrought iron during standard tests is not worse than that of mild steel. By considering appropriate values for Young's modulus and yield stress as well as the rolling direction, wrought iron bridges can be assessed in the same manner as mild steel bridges.

References

1. BRÜHWILER E., SMITH I.F.C., HIRT M.A.; Fatigue and Fracture of Riveted Bridge Members, Journal of Structural Engineering, No.1, 1990.

2. MANG F., BUCAK Ö., Remaining Fatigue Life of old Steel Bridges- Theoretical and Experimental Investigations on Railway Bridges, International Symposium on Fatigue and Fracture in Steel and Concrete Structures, India, 1991.

3. HABEL W., HOFMANN D.; Application of fibre- optic sensors for measurements and for damage detection on structures; Int. Symposium Non- Destructive- Testing in Civil Engineering, 1995.

4. HERTER J., Versuchsgestützte Tragwerksanalyse von alten genieteten Stahlbrücken zur Bewertung der Restnutzungsdauer, Kolloquium TU Berlin 11/1996.

5. BRANDES K., HELMERICH R., HERTER J., Umfassende Diagnostik für die Bewertung und Erhaltung alter Stahlbrücken, GESA Symposium 1996